

## Article

# Vanadium Complexes with Thioanilide Derivatives of Amino Acids: Inhibition of Human Phosphatases and Specificity in Various Cell Models of Metabolic Disturbances

Grzegorz Kazek <sup>1\*</sup>, Monika Głuch-Lutwin <sup>2</sup>, Barbara Mordyl <sup>2</sup>, Elżbieta Menaszek <sup>3</sup>, Monika Kubacka <sup>4</sup>, Anna Jurowska <sup>5</sup>, Dariusz Cież <sup>6</sup>, Bartosz Trzewik <sup>6</sup>, Janusz Szklarzewicz <sup>5</sup> and Monika Papież <sup>3</sup>

<sup>1</sup> Department of Pharmacological Screening, Chair of Pharmacodynamics, Faculty of Pharmacy, Jagiellonian University Medical College, Medyczna 9, 30-688 Krakow, Poland; grzegorz.kazek@uj.edu.pl

<sup>2</sup> Department of Radioligands, Chair of Pharmacobiology, Faculty of Pharmacy, Jagiellonian University Medical College, Medyczna 9, 30-688 Krakow, Poland; monika.gluch-lutwin@uj.edu.pl; barbara.mordyl@uj.edu.pl

<sup>3</sup> Department of Cytobiology, Chair of Pharmacobiology, Faculty of Pharmacy, Jagiellonian University Medical College, Medyczna 9, 30-688 Krakow, Poland; elzbieta.menaszek@uj.edu.pl; monika.papiez@uj.edu.pl

<sup>4</sup> Chair of Pharmacodynamics, Faculty of Pharmacy, Jagiellonian University Medical College, Medyczna 9, 30-688 Krakow, Poland; monika.kubacka@uj.edu.pl

<sup>5</sup> Coordination Chemistry Group, Faculty of Chemistry, Jagiellonian University, Gronostajowa 2, 30-387, Krakow, Poland; jurowska@chemia.uj.edu.pl; szklarze@chemia.uj.edu.pl

<sup>6</sup> Department of Organic Chemistry, Faculty of Chemistry, Jagiellonian University, Gronostajowa 2, 30-387, Krakow, Poland; ciez@chemia.uj.edu.pl; trzewik@chemia.uj.edu.pl

\* Correspondence: grzegorz.kazek@uj.edu.pl

**Abstract:** In the text, the synthesis and characteristics of the novel ONS-type vanadium(V) complexes with thioanilide derivatives of amino acids are described. They have shown inhibition of human protein tyrosine phosphatases (PTP1B, LAR, SHP1 and SHP2) in the submicromolar range, as well as inhibition of non-tyrosine phosphatases (CDC25A and PPA2) similar to bis(maltolato)oxovanadium(IV)(BMOV). The ONS complexes increased [14C]-deoxy-D-glucose transport into C2C12 myocytes, and one of them, VC070, also enhanced this transport in 3T3-L1 adipocytes. These complexes inhibited gluconeogenesis in hepatocytes HepG2, but none of them decreased lipid accumulation in the non-alcoholic fatty liver disease model using the same cells. Compared to the tested ONO-type vanadium complexes with 5-bromosalicylaldehyde and substituted benzhydrazides as Schiff base ligand components, the ONS complexes revealed stronger inhibition of protein tyrosine phosphatases, but the ONO complexes showed greater activity in the cell models in general. Moreover, the majority of the active complexes from both groups showed better effects than VOSO<sub>4</sub> and BMOV. Complexes from both groups activated AKT and ERK signaling pathways in hepatocytes to a comparable extent. One of the ONO complexes, VC068, showed activity in all of the above models, also including glucose utilization in the myocytes and glucose transport in insulin-resistant hepatocytes. The discussion section explicates the results within the wider scope of the knowledge about vanadium complexes.

**Keywords:** vanadium complexes; phosphatases; in vitro; cell models; metabolic disorders; diabetes; insulin resistance; gluconeogenesis; NAFLD

## 1. Introduction

Invariably, for years, type 2 diabetes (T2D) has been described as a global, social health problem. About 10% of the population suffer from diabetes and the trend is still increasing. It is predicted that by 2035, there will be approximately 600 million diabetics worldwide [1]. A much broader and still growing health problem on a global scale consists in disorders of glucose and lipid metabolism with accompanying insulin resistance,

which may predispose patients to overweight, obesity, dyslipidemia and glucose metabolism disturbances [2-4].

Altered glucose and lipid metabolism are also key factors associated with the development of nonalcoholic fatty liver disease (NAFLD), i.e., following the recently proposed nomenclature, metabolic dysfunction-associated fatty liver disease. NAFLD is the most common liver disorder, present in approximately 25% of the population, and it is estimated that NAFLD will be the most common indication for liver transplantation by 2030 [5]. Currently no therapies are registered for the treatment of NAFLD [6].

In T2D pharmacotherapy, 56 antihyperglycemic drugs have been approved as monotherapies and combination therapies by the FDA. Despite the wide spectrum of pharmacotherapy options, a large proportion of patients have difficulties in achieving sufficient clinical improvement and reducing the risk of T2D complications. This explains the presence of almost 100 additional antihyperglycemic drugs currently being evaluated in clinical trials [7, 8]. And although vanadium compounds are not included among the main pharmacotherapeutic groups used to treat metabolic disorders, their more than 100-year history of clinical trials and a wide range of studies indicate their potential for anti-diabetic activity [9-12].

Many of vanadium compounds' mechanisms of action are similar to the mechanisms of action of registered antidiabetic drugs, as well as potential pharmacotherapeutic targets in glucose and lipid metabolism disorders [13-15]. These common pharmacological mechanisms of vanadium's effects include increasing glucose uptake into cells, improving insulin sensitivity and enhancing insulin action, involving target tissues and organs: adipose tissue, muscle, and the liver [16]. Skeletal muscles are the main organ responsible for glucose homeostasis in the body [17, 18]. Like skeletal muscle, adipose tissue and the liver play key roles in lipid and glucose metabolism, and metabolic impairment of adipocytes and hepatocytes is associated with metabolic disorders [19]. Currently available pharmacological interventions in metabolic diseases target these three tissues [19, 20].

The main and best-studied intracellular target for vanadium compounds is the protein tyrosine phosphatase 1B (PTP1B), and their inhibition allows the insulin receptor to remain activated, thereby potentiating the effect of endogenous insulin [21]. This leads to the activation of the intracellular signal pathway, the AKT and PI3K kinases (phosphatidylinositol 3-kinase) which are considered potential therapeutic targets for diabetes and other conditions associated with insulin resistance [13, 22, 23]. The molecular mechanism responsible for the insulin-like effects of vanadium compounds has been shown to involve the activation of several key components' intracellular signaling pathways, including among other things, the mitogen-activated-protein kinases (MAPKs) and extracellular signal-regulated kinase 1/2 (ERK1/2) [22, 24, 25]. These pathways are essential for controlling energy homeostasis and are related to insulin sensitivity, glucose tolerance, hepatic steatosis, obesity, and diabetes.

Vanadium compounds are also inhibitors of other phosphatases besides PTP1B that are fundamental for the function of many metabolic pathways and transcription factors with wide implications for many metabolic disorders [16, 21, 26-28]. One example consists in the Src homology-2 domain-containing phosphatases type 1 and 2 (SHP1 and SHP2) and the leukocyte common antigen-related (LAR) [29]. The receptor protein tyrosine phosphatase alpha (RPTPA) also has described implications in insulin action [30]. Vanadium compounds have been shown to inhibit not only protein tyrosine phosphatases, but also serine/threonine phosphatase activity, e.g., protein phosphatase 2A (PP2A) [31, 32]. These phosphatases are also promising targets for drug development in diabetes treatment [33, 34]. In addition, vanadium compounds are inhibitors of dual-specific phosphatases including cell division cycle 25 A phosphatase (CDC25A), which is one of the most crucial cell cycle regulators [35, 36].

The above-discussed targets and molecular mechanisms of action of vanadium may result in non-specific and multidirectional biological and pharmacological effects. Other difficulties in the development of pharmaceuticals based on vanadium also result from its

high chemical reactivity in bodily fluids as well as speciation and the lack of stable metabolites [15]. The chemical affinity of vanadium for oxygen, nitrogen, or sulfur atoms, as well as its flexibility in coordination geometry, allows it to form stable complexes or transition state complexes with many biological molecules and affects biological activity [37, 38]. It is because of these chemical properties that the search for pharmacologically active, new vanadium compounds in the form of its complexes is such a promising, main direction of research on the use of vanadium in diabetes and other diseases. Of particular importance here is the advantage of complexes over organic compounds resulting from the variability of coordination numbers, geometry, redox states, ligand substitutions and structural diversity [9, 39]. The aim of modern research in the development of pharmaceuticals based on vanadium compounds is the design, synthesis, and biological testing of organic ligands or chelators with improved properties [40, 41]. A difficult task which may yield great benefit is the development of vanadium complexes with greater specificity for biological and therapeutic targets.

Previous research by our team on vanadium complexes with potential application in metabolic disorders involved the synthesis of over a hundred new vanadium complexes from different structural groups, which have been described in publications [e.g. 42-52] and patented in part [52, 53]. For the above-mentioned 110 vanadium complexes, screening tests for antidiabetic activity *in vitro* and in three cell-based models were conducted, making our research unique and significant [54]. This allowed the selection of the most active new vanadium complexes as potential compounds for metabolic disorders. Among these complexes were the five vanadium complexes with thioanilide amino acid derivatives (ONS complexes), synthesized and described for the first time, which are the subject of this publication.

The aim of this study was to evaluate the pharmacological activity of the newly synthesized ONS complexes and their effects on the metabolic processes associated with various disturbances of glucose and lipid metabolism.

In this paper, the synthesis and the physical and chemical characteristics of the novel vanadium complexes with ONS ligands is described. For these complexes, the inhibition of human PTPs and non-tyrosine phosphatases was studied. In myocytes and adipocytes the uptake of radiolabeled glucose analog was evaluated. Additionally, the effect of vanadium complexes on glucose metabolism was also investigated by assessing glucose consumption in the skeletal muscle cell model. Moreover, the accumulation of lipids in the cell model of non-alcoholic fatty liver disease (NAFLD) and the inhibition of gluconeogenesis in hepatocytes were studied. Experiments were conducted to assess the effect of vanadium complexes on radiolabeled glucose uptake to hepatocytes, in which insulin resistance was induced by the pro-inflammatory factor TNF and hyperlipidemia. Finally, the effect on radiolabeled glucose transport under hyperinsulinemia conditions was also tested and the influence of vanadium complexes on the activity of the cellular kinases, AKT and ERK, in hepatocytes were carried out.

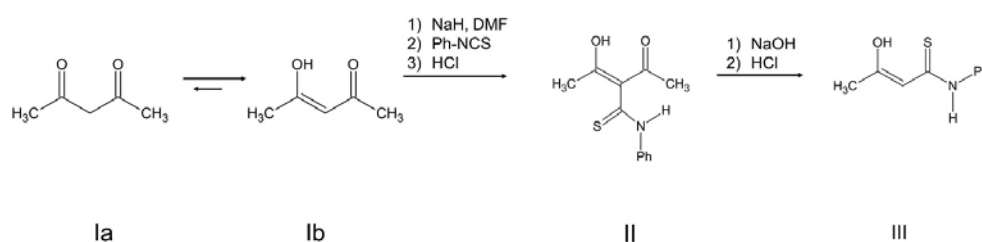
To compare the biological activity of the ONS complexes, we also conducted the tests mentioned above for the vanadium ONO complexes described previously [45-47, 55]. Compared to previously published results for these ONO complexes, the scope of research has been extended. Such an approach to the subject allowed for broader conclusions regarding the influence of the structure of vanadium complexes on biological activity.

Therefore, this study represents a continuation of our studies that used a unique screening approach to test the activity of vanadium complexes. The broad range of models and research methods used in comparison to our previous studies and those of other authors constitutes the novelty of this research.

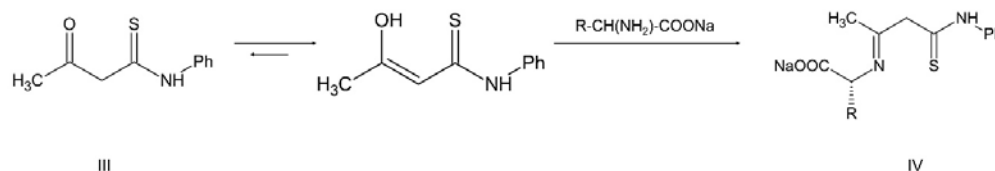
## 2. Results

### 2.1. Synthesis and characteristics of the ONS and ONO complexes

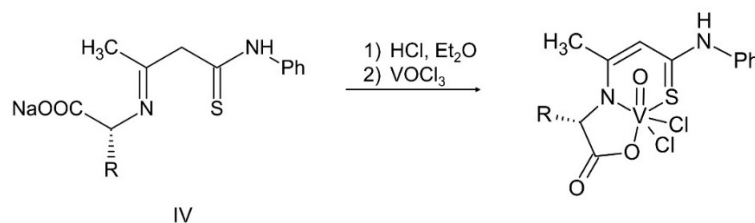
The synthesis and characterization of the ONS complexes is presented for the first time (Scheme 1-3 and Table 1). The 3-hydroxytiocrotonic acid anilide (III), as the starting compound for the preparation of ONS ligands was obtained in two steps synthesis according to Scheme 1. In the first stage, the acetylacetone in the reaction with phenyl isothiocyanate gave intermediate 2-acetyl-3-hydroxythiocrotonic acid anilide (II) which was then deacetylated to the desired 3-hydroxytiocrotonic acid anilide (III). In the next stage, the condensation reaction of (III) with appropriate L-amino acids sodium salts took place, yielding the ONS Schiff base ligands (IV) (Scheme 2). Finally, the vanadium complexes with the ONS ligands (IV) were synthesized in the reaction with vanadium(V) oxychloride ( $\text{VOCl}_3$ ) (Scheme 3).



**Scheme 1.** Two-step synthesis of 3-hydroxytiocrotonic acid anilide (III) as the starting compound for the preparation of ONS ligands.



**Scheme 2.** Condensation reaction of a thioanilide with the sodium salt of an amino acid, leading to obtaining a ligand IV with an imine structure (possible imine-enamine tautomerism). R = L-tryptophan, L-phenylalanine, L-leucine, L-methionine or D/L-isoleucine.



**Scheme 3.** Synthesis of the complexes with the ONS ligands. R = L-tryptophan, L-phenylalanine, L-leucine, L-methionine or D/L-isoleucine.

For the obtained ONS vanadium complexes (VC054, VC059, VC070, VC073 and VC0109), the formulas are presented in Table 1. These formulas are based on the results of the elemental analysis and infrared spectra (see also the *Supplementary Materials*).

Syntheses of these complexes were repeated many times, their analyzes and IR spectra were reproducible within error limits, which proves the purity of the obtained compounds and the repeatability of the syntheses.

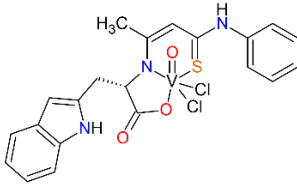
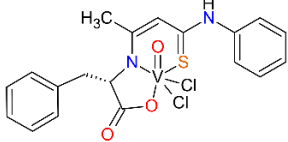
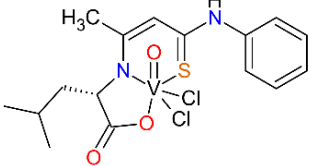
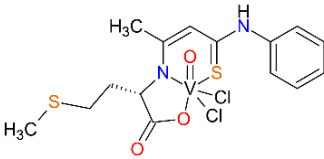
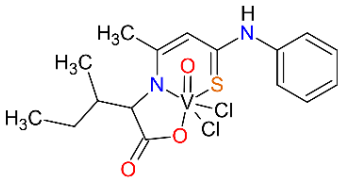
Moreover, the NMR spectra ( $^1\text{H}$ -NMR as well as  $^{13}\text{C}$ -NMR with signal assignment) of  $\text{L}_1$ - $\text{L}_5$  confirm the formation of ONS-type ligands (see the *Supplementary Materials*). The NMR spectra of ligands showed that most of the ligands, except  $\text{L}_1$  and  $\text{L}_4$ , are in the imine form. In the case of  $\text{L}_1$  and  $\text{L}_4$ , however, the imine-enamine tautomerism is quite evident in the  $^1\text{H}$ -NMR spectra: e.g. for  $\text{L}_4$  there is a small signal at 5.36 ppm from the  $=\text{CH}$ -proton, which is present in place of the  $\text{CH}_2$  protons. In addition, some other signals are doubled, which was also indicated in the description of the signal assignment. This is particularly evident in the  $\text{CH}_3$  group signal, which is doubled at 2.107 and 2.098 ppm and in the  $\text{SCH}_2$  group at 2.71 and 2.60 ppm (where there are two triplets with a mutual ratio of 4:1). This interpretation was presented under the spectra. In the  $^{13}\text{C}$ -NMR spectra of the  $\text{L}_4$  ligand, there are also some additional signals from the enamine form, but they are not as clear as in the proton spectrum.

We could not obtain a crystal suitable for single crystal X-ray measurement as the crystals formed were too small. All complexes are diamagnetic, which confirms the presence of vanadium(V). To the metal center two chlorido ligands, one oxido, and one ONS organic ligand are coordinated. However, for the biological studies described in this paper, the coordination sphere of vanadium in ONS-type complexes may not be as crucial, as the chlorido ligands are labile in the body's environment.

The ONS complexes are soluble in water and organic solvents. This may be related to the presence of chloro ligands that, when detached, can lead to the formation of an ionic complex that will be more soluble. Moreover, an increase in the ionic radius of the sulfur atom, in comparison to that of the oxygen atom, and the presence of two chloro ligands can cause stress in the coordination sphere of vanadium, leading to deformation of the structure and easier detachment of ligands, which leads to the formation of cationic complexes. The stability of the ONS complexes was tested in DMSO/ $\text{H}_2\text{O}$  (20  $\mu\text{L}$ +3 mL) and DMSO was the solvent for preparing the stock solution in pharmacological tests. Beside pH=7, the stability was tested at pH=2 condition. These complexes showed stability in this condition and at the time of incubation. Their UV-Vis spectra in solution are attached in the *Supplementary Materials*. The positions of the bands are very similar to the spectra in the DMSO itself.

In our previous studies, we described the ONO vanadium complexes. The series of the ONO vanadium complexes have been characterized in references [45-47]. Only the complex denoted as VC055 was not described; therefore, we present the synthesis and physicochemical characterization in the *Methods* section. The formulas of the vanadium complexes, the components of Schiff base ligands (used in syntheses) and the literature references are given in Figure 1 and Table 2. We selected complexes with 5-bromosalicylaldehyde and substituted benzhydrazides as components of the Schiff base ligand. For VC013, VC046, VC048, and VC050 complexes, 1,10-phenantroline (phen), as a co-ligand, stabilizes V(IV). For V(III) complexes (VC029, VC032, VC055, VC067 and VC068) two Schiff base ligands compensate the charge of the metal center. These complexes were stored under argon, but after a longer time they were oxidized to V(IV) without changing the composition of the compound, as described in our previous publications [46].

**Table 1.** The formulas of the ONS complexes with the elemental analyses and IR spectra results.

Compound	Starting amino acid	Structural formula of the complex	Elemental analysis of the complex* [%]	IR bands [cm <sup>-1</sup> ]
VC054	L-tryptophan	<div><math>[VOCl_2(L_1)] \cdot THF \cdot 6HCl</math> </div>	C, 37.38; <b>37.20</b> H, 4.86; <b>4.25</b> N, 5.22; <b>5.21</b> S, 2.91; <b>3.97</b>	3192 (w), 3054 (w), 2922 (s), 1709 (w), 1645 (s), 1619 (w), 1523 (w), 1491 (w), 1430 (m), 1396 (w), 1370 (m), 1253 (w), 1199 (w), 1120 (w), 1040 (w), 983 (m), 807 (w), 744 (m), 701 (m), 599 (w)
VC059	L-phenylalanine	<div><math>[VOCl_2(L_2)] \cdot 0.5Et_2O \cdot 1.5HCl</math> </div>	C, 44.62; <b>44.91</b> H, 4.35; <b>4.47</b> N, 4.58; <b>4.87</b> S, 5.55; <b>5.58</b>	3059 (s), 1709 (w), 1624 (s), 1606 (s), 1524 (w), 1497 (s), 1439 (m), 1407 (w), 1349 (w), 1221 (w), 1131 (w), 1078 (w), 1025 (w), 986 (m), 813 (w), 755 (m), 701 (m), 600 (w)
VC070	L-leucine	<div><math>[VOCl_2(L_3)] \cdot 2.5HCl</math> </div>	C, 36.54; <b>35.96</b> H, 4.66; <b>4.43</b> N, 4.88; <b>5.24</b> S, 5.40; <b>6.00</b>	3070 (s), 2958 (s), 1714 (w), 1618 (s), 1560 (w), 1523 (m), 1497 (s), 1447 (m), 1412 (w), 1231 (w), 1179 (w), 1120 (w), 1078 (w), 988 (m), 946 (w), 876 (w), 760 (m), 696 (m), 603 (w)
VC073	L-methionine	<div><math>[VOCl_2(L_4)] \cdot THF \cdot 2HCl</math> </div>	C, 37.29; <b>37.64</b> H, 4.79; <b>4.82</b> N, 3.98; <b>4.62</b> S, n/a	3181 (w), 3001 (s), 2921 (s), 1709 (w), 1614 (s), 1603 (s), 1560 (w), 1528 (s), 1491 (s), 1433 (s), 1346 (w), 1243 (w), 1136 (w), 1078 (w), 983 (m), 760 (m), 692 (m), 596 (w)
VC109	D/L-isoleucine	<div><math>[VOCl_2(L_5)] \cdot 3HCl</math> </div>	C, 34.77; <b>34.55</b> H, 4.38; <b>4.35</b> N, 5.07; <b>5.04</b> S, 5.80; <b>5.77</b>	3338 (w), 3059 (w), 2970 (s), 2939 (w), 2885 (w), 1729 (w), 1606 (s), 1520 (s), 1489 (s), 1447 (m), 1389 (w), 1350 (w), 1218 (w), 1180 (w), 1114 (w), 986 (m), 865 (w), 758 (m), 696 (m), 599 (w)

\* the calculated elemental analyses are in bold.



**Table 2.** The formulas of the ONO complexes and the hydrazide components of Schiff base ligands ( $L_n$ ) used in synthesis with the reference for previously described complexes; phen = 1,10-phenanthroline.

Compound	Formula	$L_n$ components (1:1 molar ratio)		Ref.
		Aldehyde	Hydrazide	
VC013	$[VO(L_6)(phen)] \cdot H_2O$	5-bromosalicyl-aldehyde	2-hydroxybenzhydrazide	[45]
VC029	$[V(L_7)(HL_7)]$		2-hydroxybenzhydrazide	[46]
VC032	$[V(L_8)(HL_8)] \cdot H_2O$		benzhydrazide	[47]
VC046	$[VO(L_9)(phen)] \cdot 2H_2O$		4-hydroxybenzhydrazide	[46]
VC048	$[VO(L_{10})(phen)] \cdot 0.5H_2O$		4-tertbutylbenzhydrazide	[47]
VC055	$[V(L_{11})(HL_{11})]$		4-methoxybenzhydrazide	-*
VC050	$[VO(L_{11})(phen)]$		4-chlorobenzhydrazide	[46]
VC067	$[V(L_{12})(HL_{12})]$		3-hydroxy-2-naphthoic acid hydrazide	[46]
VC068	$[V(L_{13})(HL_{13})]$		4-nitrobenzhydrazide	[46]

\* described in this study.

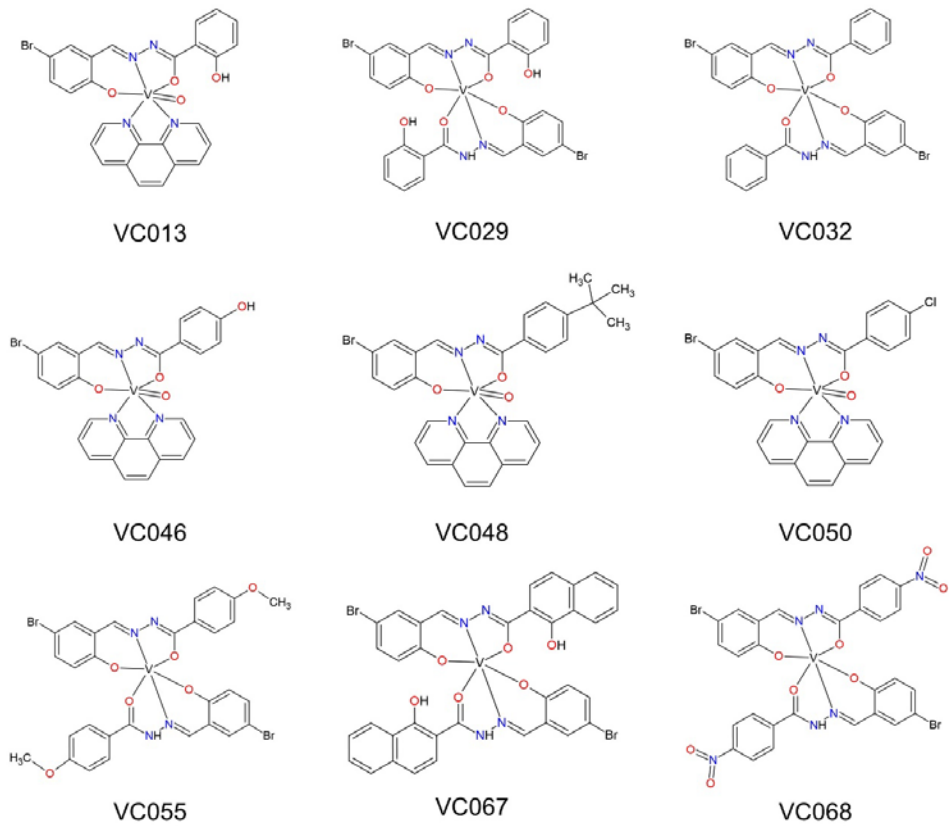


**Figure 1.** The structural formulas of the ONO complexes.

2.2. The ONS complexes inhibit the activity of human tyrosine phosphatases stronger than the ONO complexes

At first, in our screening tests we showed that ONS complexes, as well as ONO ones, at a concentration of 1  $\mu$ M, inhibited human tyrosine phosphatases PTP1B, LAR, SHP1, and SHP2; however, ONS complexes exhibited higher activity than ONO ones (Table 3). ONS complexes inhibited LAR phosphatase activity in the range of 56 to 69% relative to controls (100% activity), and the percentage inhibition of the other phosphatases was

similar, ranging from 70 to 88%. Most of the ONO complexes showed weaker inhibitory potency than the ONS complexes and comparators.

The ONO complexes exhibited significantly greater diversity in the strength of inhibition of protein tyrosine phosphatases than the ONS complexes. For instance, the highest values of PTP1B inhibition were shown by the VC013 complex, which inhibited the activity of this phosphatase by 60%, and the VC032 by 9%, was the weakest complex in the ONO group (Table 3). Aside from VC013, the other ONO complexes demonstrated higher inhibitory potency than VOSO<sub>4</sub> and BMOV. The last two were used as comparator vanadium compounds to evaluate the relative activity of the tested complexes. Suramin and ammonium heptamolybdate ((NH<sub>4</sub>)<sub>6</sub>Mo<sub>7</sub>O<sub>24</sub>) were used as control compounds, organic and inorganic non-vanadium compound, respectively.

**Table 3.** Inhibition of human tyrosine phosphatases by the ONS and ONO vanadium complexes at the concentration of 1 μM. Results are expressed as percentage of inhibition of the control (solvent only). Standard deviation did not exceed 6%.

		PTP1B	LAR	SHP1	SHP2
Non-vanadium control	Suramin	7	9	17	10
	(NH <sub>4</sub> ) <sub>6</sub> Mo <sub>7</sub> O <sub>24</sub>	33	28	40	47
Vanadium comparators	VOSO <sub>4</sub>	62	44	70	77
	BMOV	77	58	76	82
ONS complexes	VC054	78	67	84	87
	VC059	79	71	82	87
	VC070	79	69	84	88
	VC073	74	63	82	86
	VC109	70	56	80	83
ONO complexes	VC013	60	66	67	74
	VC029	31	25	62	68
	VC032	9	8	44	48
	VC046	34	37	62	66
	VC048	36	35	62	64
	VC050	25	19	53	57
	VC055	24	18	56	57
	VC067	42	39	70	74
	VC068	40	33	70	74

The backgrounds of the table cells represent a two-color scale heat map. The darkest red would indicate 100% inhibition, the darkest blue would indicate 0%, and the middle of the scale, corresponding to 50% inhibition, is colorless.

In the next step, we confirmed the effects observed in the screening tests by determining the IC<sub>50</sub> for selected complexes from both groups (Table 4). To determine the IC<sub>50</sub>, the ONO complexes were selected, which had shown significant biological activity in our previous studies [46], despite not demonstrating the highest inhibition in screening assays. For all tested phosphatases, the IC<sub>50</sub> values obtained for ONS complexes were similar to IC<sub>50</sub> values for VOSO<sub>4</sub> and BMOV. However, ONO complexes showed approximately 30-40 times weaker inhibition than ONS complexes and comparators (Table 4).



Ammonium heptamolybdate ((NH<sub>4</sub>)<sub>6</sub>Mo<sub>7</sub>O<sub>24</sub>) was used as non-vanadium, inorganic control compound.

**Table 4.** Inhibition of the human tyrosine phosphatases by the selected ONS and ONO complexes.

		IC50 [nM]				Log IC50±SD			
		PTP1B	LAR	SHP1	SHP2	PTP1B	LAR	SHP1	SHP2
Non-vanadium control	(NH <sub>4</sub> ) <sub>6</sub> Mo <sub>7</sub> O <sub>24</sub>	58	38	26	26	-7.24±0.06	-7.42±0.04	-7.59±0.13	-7.58±0.04
Vanadium comparators	VOSO <sub>4</sub>	99	95	17	13	-7.00±0.07	-7.88±0.10	-7.77±0.02	-7.77±0.02
	BMOV	149	140	14	8	-6.83±0.02	-8.09±0.11	-7.86±0.03	-7.86±0.03
ONS complexes	VC054	141	112	20	20	-6.85±0.01	-7.70±0.06	-7.56±0.02	-7.56±0.02
	VC059	107	76	26	13	-6.97±0.01	-7.87±0.06	-7.59±0.04	-7.59±0.04
ONO complexes	VC050	4263	1714	657	273	-5.37±0.03	-6.56±0.04	-6.18±0.03	-6.18±0.03
	VC068	2034	619	517	235	-5.69±0.02	-6.63±0.03	-6.29±0.02	-6.29±0.02

2.3. The ONS and ONO complexes are inhibitors of non-tyrosine phosphatases

The ONS and ONO complexes also showed inhibition of non-tyrosine phosphatases: CDC25A dual specificity phosphatase and PPA2 serine-threonine phosphatase in a range similar to that of VOSO<sub>4</sub> and BMOV (Table 5). The exception was VC050 which at the concentration of 1 µM showed weaker inhibition than the other complexes and comparators. VC050 also showed less activity on inhibition tyrosine phosphatases as shown above.

**Table 5.** Inhibition of human non-tyrosine phosphatases and PTPRA by the selected ONS and ONO complexes. Results are expressed as percentage inhibition of control (solvent only) ±SD.

		CDC25A		PP2A	
		10 µM	1 µM	10 µM	1 µM
Non-vanadium comparator	(NH <sub>4</sub> ) <sub>6</sub> Mo <sub>7</sub> O <sub>24</sub>	51±1	34±1	53±3	18±2
Vanadium comparators	VOSO <sub>4</sub>	62±1	54±2	40±3	32±2
	BMOV	61±1	54±1	63±4	52±15
ONS complexes	VC054	65±3	51±2	75±7	41±15
	VC059	68±3	55±3	54±9	44±1
ONO complexes	VC050	38±1	12±8	51±4	24±3
	VC068	62±2	54±3	55±15	26±12

2.4. The ONS complexes enhance glucose transport into myocytes and adipocytes to a lesser extent than ONO complexes

At the concentration of 50 µM, ONS complexes caused an increase in the transport of [14C]-deoxy-D-glucose into C2C12 myocytes in the range of 119-158% of the control. VOSO<sub>4</sub> and BMOV showed an increase of transport to 110% and 125% of the control, respectively, with statistical significance only for BMOV (Figure 2). On the other hand, the observed effect of ONO complexes on [14C]-deoxy-D-glucose transport was significantly greater than that of ONS complexes. ONO complexes

significantly enhanced transport, from 199% to 267% of the control with statistical significance between  $p \leq 0.001$  and  $p < 0.05$ . VC032, the most active complex at the concentration of 50  $\mu\text{M}$  also showed significant effects at concentrations of 10 and 1  $\mu\text{M}$ , indicating a concentration-dependent response.

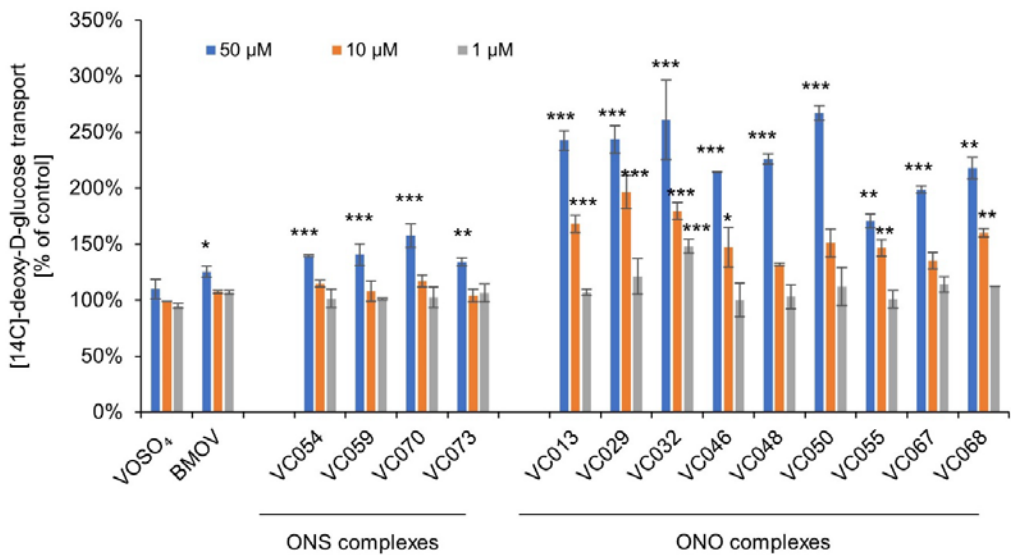


**Figure 2.** The effect of vanadium complexes on the transport of [14C]-deoxy-D-glucose into myocytes C2C12. The results are presented as a percentage of the control cells treated with the solvent only (mean  $\pm$  SD). Statistical significance vs. control is denoted as \* $p \leq 0.05$ , \*\* $p \leq 0.01$ , \*\*\* $p \leq 0.001$ . Results for VC029, VC046, VC050, VC067, and VC068 were previously published by us in [46].

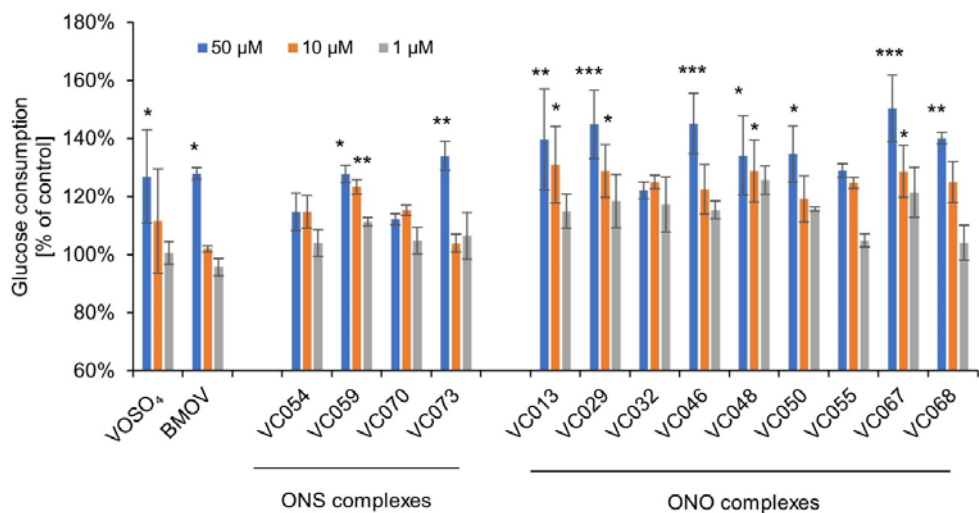


**Figure 3.** The effect of vanadium complexes on glucose consumption by myocytes C2C12. The results are presented as a percentage of the control cells treated with the solvent only (mean  $\pm$  SD). Statistical significance vs. control is denoted as \* $p \leq 0.05$ , \*\* $p \leq 0.01$ , \*\*\* $p \leq 0.001$ .

At the highest tested concentration, the ONS complexes increased glucose consumption by myocytes C2C12 in the range 104 to 134% of the control value (Figure 3).

The ONO complexes at the concentration of 50  $\mu$ M increased glucose consumption within a range of 122 to 150% compared to the control ( $p \leq 0.001$  to 0.05). No statistically significant effect was observed only for VC032 and VC055.

Simultaneously with glucose consumption tests, the viability of myocytes C2C12 was examined due to their prolonged, 24-hour incubation with vanadium complexes. Cell viability was not lower than 80% of the vehicle control for all tested complexes, which is recognized as a lack of cytotoxic effect [56]. After incubation with the tested complexes at a concentration of 50  $\mu$ M, the lowest viability was observed for VC054 ( $84 \pm 8\%$ ) and VC059 ( $86 \pm 6\%$ ), while it was  $90 \pm 4\%$  for BMOV. For some complexes, as well as the rosiglitazone used as a reference compound, an increase in the signal was observed (e.g., VC055  $127 \pm 5\%$  and rosiglitazone  $120 \pm 7\%$ ) [47].

Among the ONS complexes, only VC070 enhanced the transport of [14C]-deoxy-D-glucose into 3T3-L1 adipocytes (159% of control at 50  $\mu$ M,  $p \leq 0.001$ ; Figure 4). This complex also exhibited the strongest effect on radiolabeled deoxy-D-glucose transport into C2C12 myocytes. The remaining ONS complexes did not significantly affect this transport (92–107% of control at 50  $\mu$ M,  $p > 0.05$ ). Similarly, the comparators BMOV and VOSO<sub>4</sub> showed low activity in comparison to the control.

For the ONO complexes, two of them did not affect the transport of [14C]-deoxy-D-glucose into 3T3-L1 adipocytes: VC032 and VC067 (Figure 4). The rest of the complexes in this group intensified this transport in a range of 134 to 177% of control, with statistically significant activity at a concentration of 50  $\mu$ M observed for complexes VC013, VC029, and VC068 ( $p \leq 0.001$ ).

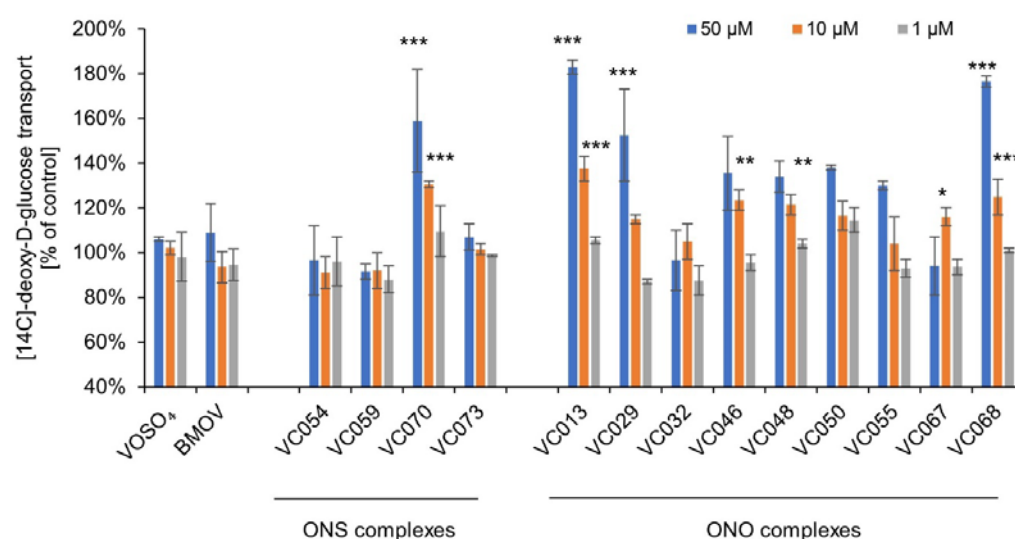


**Figure 4.** The effect of vanadium complexes on the transport of [14C]-deoxy-D-glucose into adipocytes 3T3-L1. The results are presented as a percentage of the control cells treated with the solvent only (mean  $\pm$  SD). Statistical significance vs. control is denoted as \* $p \leq 0.05$ , \*\* $p \leq 0.01$ , \*\*\* $p \leq 0.001$ . Results for VC029, VC046, VC050, VC067, and VC068 were previously published by us in [46].

It is noteworthy that both groups of complexes exhibited differential effects on the transport of [14C]-deoxy-D-glucose in the above cellular models (myocytes vs. adipocytes). Among ONS complexes, only VC070 showed activity in both models (myocytes C2C12  $158 \pm 10\%$  and adipocytes 3T3-L1  $159 \pm 14\%$  of control). The rest of complexes in this

group did not demonstrate significant activity in adipocytes 3T3-L1 (92%-107% of control,  $p>0.05$ ). The ONO complexes, VC032 and VC067 enhanced the transport of [14C]-deoxy-D-glucose only in myocytes C2C12, without exhibiting similar activity in adipocytes 3T3L-1. VC032 caused an increase of this transport into myocytes ( $266\pm36\%$  of control) and no effects in adipocytes ( $97\pm14\%$ ; t-test,  $p=0.04$ ). For VC067, these values were  $199\pm3\%$  and  $94\pm14\%$  for myocytes and adipocytes, respectively (t-test,  $p=0.0002$ ). The differences in the activity of the other tested ONO complexes did not show statistically significant differences (t-test,  $p>0.05$ ).

### 2.5. The ONO complexes but not the ONS complexes reduce hepatocyte steatosis in the cellular model of non-alcoholic fatty liver disease (NAFLD)

In the cellular model of hepatic steatosis, the ONS complexes showed no effect on the amount of lipid accumulation after induction of hepatocytes steatosis with oleic acid (90-116% of control,  $p>0.05$ ; Figure 5). Similarly, the comparators VOSO<sub>4</sub> and BMOV did not have any significant effect in comparison to the control.

Two ONO complexes showed very distinct effects. The accumulation of lipids in hepatocytes was 52% and 36% lower for VC067 and VC068, respectively, compared to the control ( $p\leq0.001$ ) (Figure 5). The ONO complexes, VC029, VC032, and V050, caused a large and statistically significant increase in lipid accumulation in hepatocytes (from 128% to 151% of control,  $p\leq0.001$  for VC050 and  $p\leq0.01$  for the other two complexes). This may be due to an undesirable effect on metabolic mechanisms or a hepatotoxic effect resulting in hepatocyte steatosis, without damage or reducing the number of hepatocytes [57].

We conducted cytotoxicity studies on the same hepatocytes used to measure lipid accumulation after incubation with the tested complexes. We also conducted simultaneous analysis of cell membrane integrity. Assays showed no significant differences from controls for any of the tested ONS and ONO complexes; therefore, the effect of reducing intracellular lipids should not be attributed to a reduction in cell number due to a cytotoxic effect.

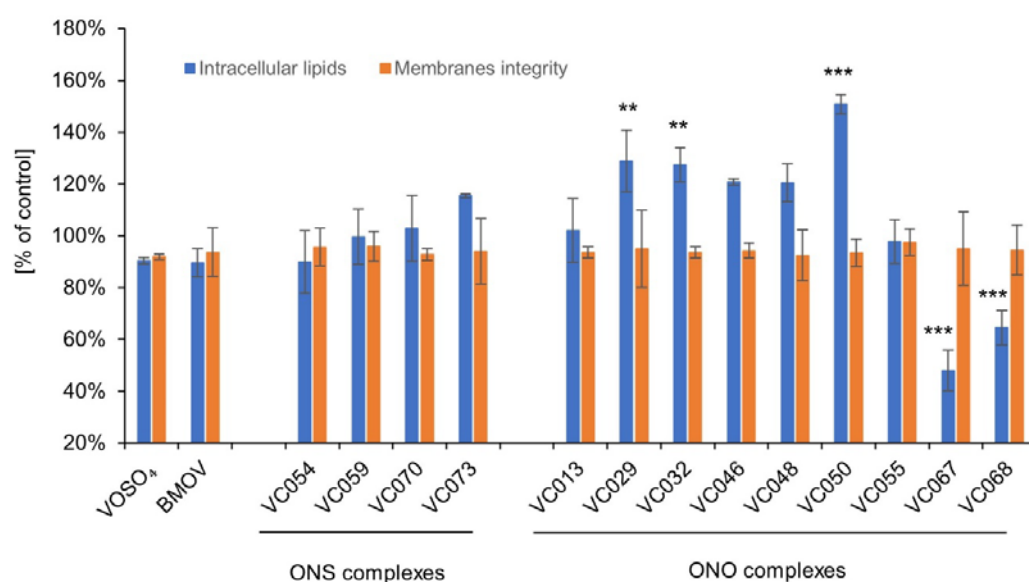


**Figure 5.** The effect of incubation of the vanadium complexes (10  $\mu$ M) during induction steatosis on the accumulation of intracellular lipid and cytotoxicity in hepatocytes HepG2. The results are presented as a percentage of the control cells treated with the solvent only (mean  $\pm$  SD). Statistical significance vs. control is denoted as \* $p\leq0.05$ , \*\* $p\leq0.01$ , \*\*\* $p\leq0.001$ .

### 2.6. The ONS and the ONO complexes inhibit gluconeogenesis in hepatocytes

Continuing the research on the effects on the hepatic mechanisms of metabolic disorders, studies were conducted on the effect of selected ONS and ONO complexes on gluconeogenesis in HepG2. Among them were the ONO complexes VC067 and VC068, which showed inhibition of lipid accumulation in the same cells.

All the tested complexes of both types and BMOV at the concentration of 50  $\mu$ M showed potent and statistically significant inhibition of glucose synthesis in hepatocytes, ranging from 46 to 81% of control (Figure 6). Known inhibitors of gluconeogenesis, metformin (a first-line treatment for type 2 diabetes), insulin, and AICAR (5-aminoimidazole-4-carboxamide riboside) as an AMPK activator inhibiting transcription of the gluconeogenesis genes were used as the experimental control. All the control compounds showed inhibition of glucose synthesis by hepatocytes.

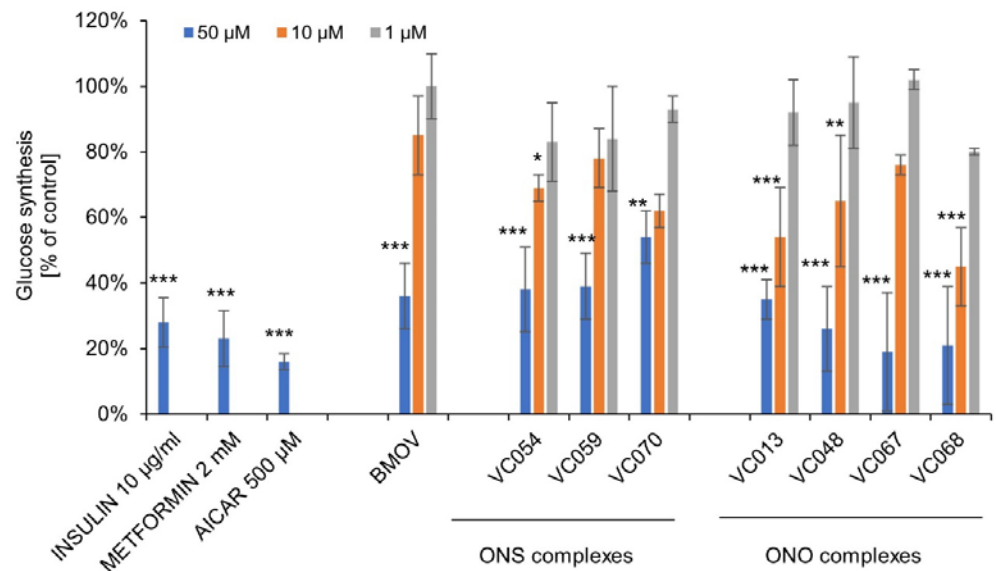


**Figure 6.** The effect of the vanadium complexes on gluconeogenesis in hepatocytes HepG2. The results are presented as a percentage of the control cells treated with the solvent only (mean  $\pm$  SD). Statistical significance vs. control is denoted as \* $p \leq 0.05$ , \*\* $p \leq 0.01$ , \*\*\* $p \leq 0.001$ .

### 2.7. The ONO complexes reverse the impairment of glucose transport to hepatocytes under conditions of insulin resistance and hyperinsulinemia

Insulin resistance of HepG2 hepatocytes was induced in two ways: by preincubating them with the proinflammatory cytokine TNF and with oleic acid, which in both cases resulted in a decrease in [14C]-deoxy-D-glucose transport (Figure 7). Then, these hepatocytes were incubated with the ONO complexes, VC067 and VC068, which most effectively among the tested complexes reduced lipid accumulation and inhibited gluconeogenesis in the same cells.

At the concentration of 10  $\mu$ M, the VC067 complex reversed the decrease in [14C]-deoxy-D-glucose transport in hepatocytes in which insulin resistance was induced by oleic acid, and the VC068 complex reversed the decrease in transport induced by TNF ( $p \leq 0.05$ ). The observed effects were greater than those for 1 mM metformin.

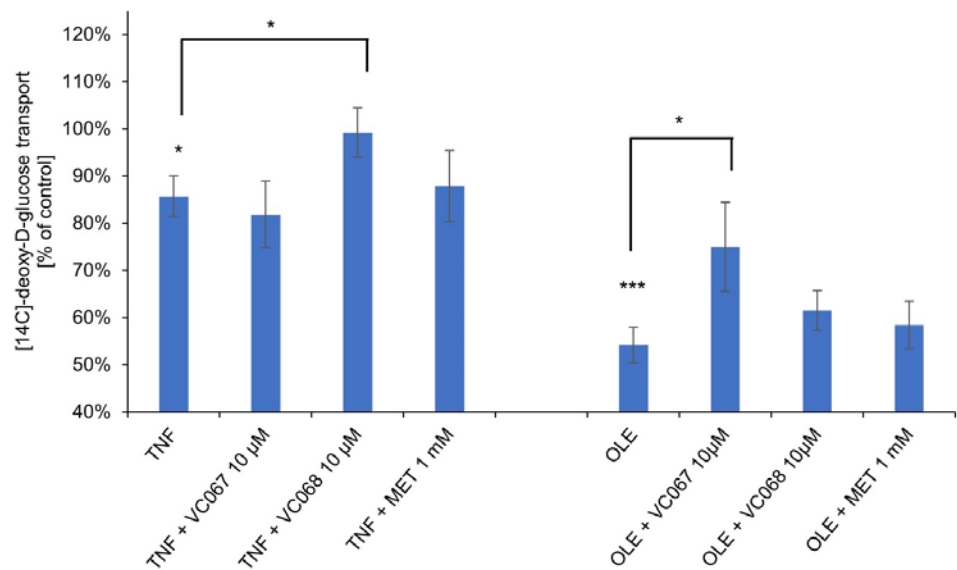


**Figure 7.** The effect of vanadium complexes on the transport of [14C]-deoxy-D-glucose into hepatocytes HepG2, in which insulin resistance was induced by preincubation with TNF and oleic acid (OLE). MET – metformin. The results are presented as a percentage of the control cells treated with the solvent only (mean ± SD). Statistical significance is denoted as \*p≤ 0.05, \*\*p≤ 0.01, \*\*\*p≤ 0.001. For TNF and OLE statistical significance vs. control cells.

The complexes did not potentiate the transport of [14C]-deoxy-D-glucose to hyperinsulinemia-induced insulin-resistant hepatocytes at 10 µM, nor did metformin at 1 mM (Figure 8). Insulin resistance of hepatocytes was only reversed by very high concentrations of insulin (10 µg/mL).

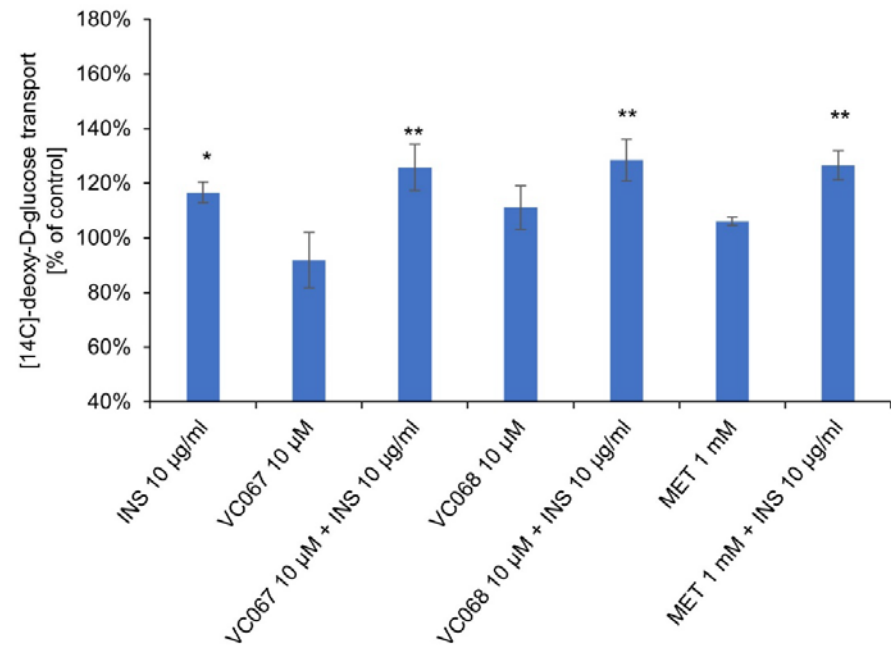


**Figure 8.** The effect of vanadium complexes on the transport of [14C]-deoxy-D-glucose into hepatocytes HepG2, in which insulin resistance was induced by preincubation with insulin (INS). CON – control, MET – metformin. The results are presented as a percentage of the control cells treated with the solvent only (mean ± SD). Statistical significance vs. control is denoted as \*p≤ 0.05, \*\*p≤ 0.01, \*\*\*p≤ 0.001. For insulin statistical significance vs. control insulin resistant cells.



### 2.8. The ONS and ONO complexes activate ERK and AKT signaling pathways

For the selected ONS and ONO complexes, studies on the effect on the phosphorylation of AKT and ERK kinases as molecular targets of insulin and vanadium compounds were performed. Under the influence of the tested complexes at a concentration of 50  $\mu\text{M}$ , an increase in the level of AKT phosphorylation in HepG2 hepatocytes was observed, in the range of 117-168% of the control after 1 hour and in the range of 112-138% of the control 3 hours after the end of cell exposure (Figure 9). Human insulin was used as the experiment control for AKT activation. Wortmannin, a PI3K inhibitor, and triciribine, a highly selective AKT inhibitor, were used for inhibition of insulin effects on AKT.

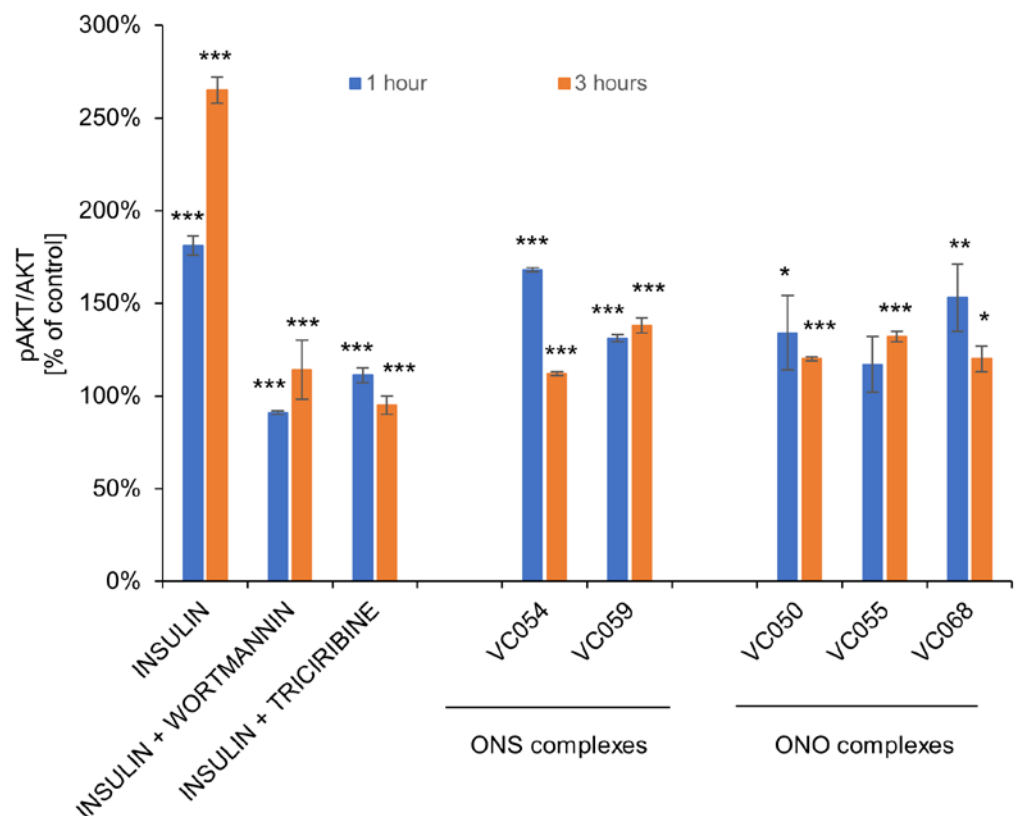


**Figure 9.** The effect of the vanadium complexes on AKT(Thr308) phosphorylation in HepG2 hepatocytes. The results are presented as a percentage of the pAKT/AKT ratio against control cells treated with the solvent only (mean  $\pm$  SD). Human insulin was used at a concentration of 10  $\mu\text{g}/\text{ml}$ , wortmannin at 1  $\mu\text{M}$ , and triciribine at 10  $\mu\text{M}$ . Statistical significance vs. control is denoted as \* $p \leq 0.05$ , \*\* $p \leq 0.01$ , \*\*\* $p \leq 0.001$ . For insulin with AKT inhibitors, statistical significance vs. insulin alone.

All of the tested complexes also enhanced ERK phosphorylation. Human insulin was used as positive control for ERK fosforylation. FR180204, a selective ERK inhibitor and PD98053, an MEK inhibitor, were used as control compounds for inhibition of the insulin effects (Figure 10).

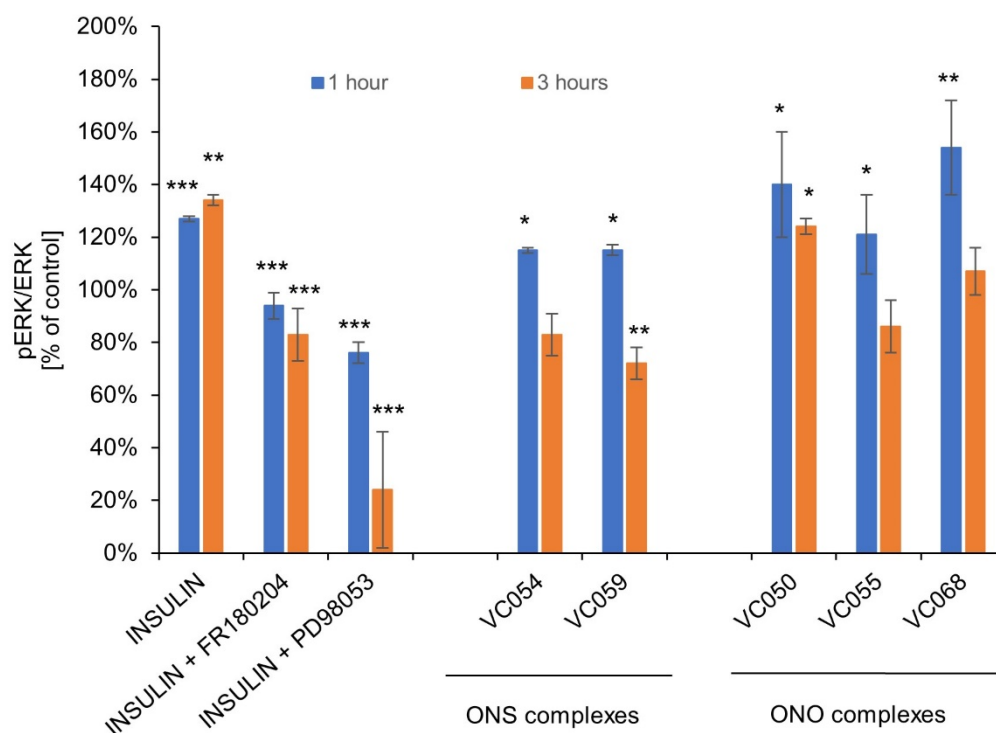


**Figure 10.** The effect of the vanadium complexes on ERK1/2 (Thr202/Tyr204) phosphorylation in HepG2 hepatocytes. The results are presented as a percentage of the pERK/ERK ratio against control cells treated with the solvent only (mean  $\pm$  SD). Human insulin was used at a concentration of 10  $\mu$ g/ml, FR180204 at 2  $\mu$ M, and PD98053 at 50  $\mu$ M. Statistical significance vs. control is denoted as \* $p \leq 0.05$ , \*\* $p \leq 0.01$ , \*\*\* $p \leq 0.001$ . For insulin with ERK inhibitors, statistical significance vs. insulin alone.

### 3. Discussion

Most studies have analyzed the antidiabetic effects of vanadium complexes in a narrow and limited scope, despite the complex mechanisms underlying this activity. Only a wide range of studies can reveal the full potential of the therapeutic possibilities of vanadium complexes, and this is the approach we used in our work. We conducted *in vitro* studies of human phosphatases inhibition and we used various cell models of organs and tissues connected with the pathogenesis of metabolic disorders: myocytes, adipocytes and hepatocytes. In these models, we studied numerous processes related to the pharmacotherapy of metabolic disorders: glucose transport and its utilization, as well as lipid accumulation, gluconeogenesis, and insulin resistance in hepatocytes. Importantly, we studied the effects of vanadium targeting not only diabetes itself, but also other metabolic disorders associated with or leading to diabetes.

Searching for new vanadium complexes with better properties and biological effectiveness, we synthesized new complexes with thioanilide amino acid derivatives. We decided to use ONS ligands, comparing them with ONO ligands to check whether the change of one oxygen into one sulphur atom in the first coordination sphere influences biological activity. To have very similar complexes, five and six-membered rings should be formed. Therefore, we used thioanilide as a six-membered component and an analogue of the salicylaldehyde used in ONO-type complexes. Amino acids were used due to the presence of the  $\text{NH}_2$  group that can form an imine bond with the carbonyl group of the thioanilide. Additional a  $\text{COO}^-$  group of amino acids has a donor oxygen atom in the

appropriate position to form a five-membered ring with a central vanadium atom. Moreover, the presence of sodium salts formed of amino acids increased the solubility of the obtained vanadium complexes, which is important from the point of view of the compound's bioavailability. When comparing the biological activity of complexes with ONO- and ONS-type ligands, in the presence of a sulfur atom, electron polarization is easier, which leads to stabilization of the 5th oxidation state of vanadium. The influence of the substituents in the ONS Schiff base ligand on biological activity is not as significant as in the case of the ONO-donor ligands. The results of pharmacological tests for the ONS complexes are more comparable within this group, in contrast to the ONO complexes.

Orthovanadate ( $\text{VO}_4^{3-}$ ), as a biologically active part of complexes of vanadium and other organovanadium compounds, are considered non-selective, competitive, reversible inhibitors of tyrosine phosphatases [16, 21, 28, 58, 59]. Some vanadium compounds, for example, peroxyvanadium complexes, are capable of oxidizing cysteine residues in the critically active site of phosphatases, which results in irreversible inhibition of enzymatic activity [21]. In this way, vanadium exhibits a broad inhibitory capacity on the entire superfamily of tyrosine phosphatases, which has been experimentally demonstrated using panels of various tyrosine phosphatases, such as PTP1B, SHP1, SHP2, TCPTP, PTP-MEG2, HePTP, HCPTPA, and HPTPb [58, 60-63].

Despite initially being considered a non-selective inhibitor of tyrosine phosphatases, various studies have indicated the possibility of the more selective action of vanadium complexes. A review containing a compilation of results for the inhibition of different tyrosine phosphatases by several vanadium complexes indicated that they may exhibit varying degrees of inhibition [28]. In this compilation, some complexes showed 3 to 50 times stronger inhibition of PTP1B than other tyrosine phosphatases, while others showed no or little difference in inhibiting phosphatases other than PTP1B [60].

Most attention is paid to the importance of PTP1B phosphatase in diabetes and metabolic disturbances. However, ample evidence points to the important role of other tyrosine phosphatases in these disorders. Results suggest that SHP1 may be a potential target for muscle insulin resistance, insulin signalling during obesity, and may be involved in the development of non-alcoholic fatty liver disease caused by diet-induced obesity [64-66]. Similarly, inhibition of SHP2 has been implicated in various signalling pathways, including those involved in potential anti-diabetic actions. The effect of inhibition decreased insulin resistance, decreased liver steatosis, enhanced insulin-induced suppression of hepatic glucose production, and impeded the development of insulin resistance after high-fat feeding [67-69]. Regarding LAR, the results indicate its involvement in the pathogenesis of metabolic disorders and suggest this phosphatase as a potential therapeutic target [70-72].

We have conducted studies on the inhibition of human recombinant PTP1B, the most extensively described biological target for vanadium activity, as well as on highly homologous human tyrosine phosphatases, such as LAR, SHP1, and SHP2, which may have potential relevance in metabolic diseases [27, 29].

Screening tests and determination of  $\text{IC}_{50}$  confirmed that all ONS complexes are inhibitors of all tested phosphatases at a similar level to  $\text{VOSO}_4$  and BMOV. The rationale for employing these last two compounds as comparators of biological activity is grounded on their extensive research history and their established effectiveness in metabolic disorders. The absence of a comparator in most published studies poses challenges in comparing the relative activity of the studied vanadium compounds. Moreover, the published results of inhibition tests cover a wide range of results, for example  $\text{IC}_{50}$  for PTP1B for  $\text{VOSO}_4$  ranges from 18 nM [73] to 380 nM [74]. This can be explained by differences in the substrate used (e.g., DiFMUP vs. p-NPP) or other analytical conditions. Our results for BMOV are consistent with previously published results of other authors ( $\text{IC}_{50}$  for PTP1B was 0.15  $\mu\text{M}$ ) [58]. Similarly, ONS complexes exhibit a comparable level of potency in inhibitory activity ( $\text{IC}_{50}$  was 0.14 and 0.11  $\mu\text{M}$  for VC054 and VC059, respectively). The

obtained results for the inhibition of other tested phosphatases align with the values reported in the literature, which commonly fall within the IC<sub>50</sub> range of 0.1-0.9  $\mu$ M [28].

The ONO complexes exhibited approximately 15-30 times weaker inhibition of PTP1B compared to BMOV and the ONS complexes. Similarly, the inhibition of the other tested tyrosine phosphatases was even several dozen times weaker for the ONO complexes. The comparators, BMOV and VOSO<sub>4</sub>, commonly used in previously published studies, exhibit a greater inhibitory effect on PTP1B than on SHP1 and SHP2. However, conflicting results have been reported by certain authors [75]. The differences in the activity of these comparators are small enough that VOSO<sub>4</sub> and BMOV are reported to be non-selective for these tyrosine phosphatases. Referring to these data, our results for comparators as well as the studied complexes suggest that the differences in the tyrosine phosphatase inhibition strength may rather result from analytical conditions, such as different specific activity of the recombinant enzyme used for the analyses. Moreover, the presence of EDTA or a thiol-containing reducing agent (e.g., DDT), which modulates the catalytic activities of PTP1B and SHPs, may play a crucial role in modifying the complexes present in the reaction environment and determining the result [75].

The tested ONS and ONO complexes showed inhibition of human non-tyrosine phosphatases: dual specificity phosphatase CDC25A and serine-threonine phosphatase PPA2. Very few publications on the biological activity of vanadium include the study of phosphatases from other classes and groups with different substrate specificity, such as CDC25A, which is the oncoprotein regulating the cell cycle [76-78]. Orthovanadate can inhibit the activity of calcineurin, a serine/threonine protein phosphatase that plays a crucial role in numerous signal transduction pathways [31, 79]. Our results for PP2A are consistent with these findings and confirm that vanadium complexes inhibit not only protein tyrosine phosphatases, but also serine/threonine phosphatases. Although few studies on the activity of vanadium compounds include these phosphatases, this direction seems important because over 98% of protein phosphorylation occurs on serine and threonine residues, and specific serine/threonine phosphatases are important and promising targets for drug development, particularly in diabetes treatment [33]. On the other hand, the non-specific effect of vanadium on phosphatases involved in cell cycle regulation may be a limitation of the clinical use of vanadium compounds in non-malignant diseases.

The ONS complexes showed higher activity in inhibiting human tyrosine phosphatases than the ONO complexes; however, it is interesting that their biological activity in cellular models of skeletal muscle and adipose tissue is lower than that of the ONO complexes. Similar results were observed, for example, for the ((CH<sub>3</sub>)<sub>2</sub>NO)<sub>2</sub>V(O)OH complex, which was not as good a PTPs inhibitor as vanadate, but was much more effective in inducing biological effects in cells by means of increasing glucose transport and glycogen synthesis [80].

We used the cell models of the main organs responsible for glucose metabolism, which are also target organs for diabetes pharmacotherapy. C2C12 myoblasts are a well-documented model with key characteristics of human muscle cells. This model is widely used in preclinical and pharmacological studies in the development of new drugs [81-83], including vanadium compounds [85-87]. Adipocytes of the 3T3-L1 line, also used in research on vanadium compounds, are similarly useful for the same reasons [87, 88]. Impairment of insulin signaling and post-receptor intracellular mechanisms in insulin resistance is manifested by reduced glucose transport to myocytes and adipocytes, and its improvement is one of the main pharmacotherapeutic mechanisms in diabetes treatment [89, 90]. In our study we used radioactively labeled deoxy-D-glucose, a synthetic glucose analogue, which is transported to cells but does not undergo further metabolism in the glycolysis process. The product of the first stage of glycolysis inhibits this process non-competitively.

Different vanadium compounds, including its complexes, have an effect on basal and insulin stimulated glucose uptake in adipocytes [91, 92] as well as in myocytes [84-86]. Our ONS and ONO complexes also increased transport of [14C]-deoxy-D-glucose into

myocytes C2C12. Compared to the ONO complexes, the activity of the ONS complexes was lower, but despite this, they showed greater efficiency than  $\text{VOSO}_4$  and BMOV.

We extended the study of the transport of radiolabeled glucose analog to C2C12 myocytes with the study of glucose utilization (consumption) during a 24-hour incubation with vanadium complexes. The study of glucose consumption gives a more complete picture of the pharmacological activity of the tested complexes because it depends on its consumption in cells, e.g., in the process of glycogenesis. In patients with type 2 diabetes, increased glycogen synthesis after administration of  $\text{VOSO}_4$  accounted for more than 80% of the increased glucose disposal in muscles [93]. In this case, the stimulation of glucose uptake by myocytes is independent of the effect of vanadium on the insulin receptor signal through the inhibition of tyrosine phosphatases [94]. We did not find any studies in which both glucose transport and glucose utilization were studied in the same cell model.

As in the study of the transport of [14C]-deoxy-D-glucose in myocytes C2C12, the ONS complexes also showed a lower effect on glucose utilization than the ONO complexes. These effects were greater than those of  $\text{VOSO}_4$  and BMOV. In the experiment investigating glucose consumption by myocytes, no differences in activity were observed between the ONS and ONO complexes, in contrast to differences in the increase of [14C]-deoxy-D-glucose transport in the same cells.

Biotransformation of the complexes and vanadium speciation may be a possible cause. These processes can be critical to the observed activity and depend on the experimental condition and the time of incubation with the complexes, which in the study of the glucose analog transport to C2C12 myocytes was 6 hours in total, and in the study of glucose consumption by these cells was 24 hours. Biological activity depending on the incubation time has been demonstrated, among other things, in the case of vanadium complexes with 1,10-phenanthroline ligands. After 3 and 24 hours, the cytotoxicity was different for the tested complexes, but after 72 hours of incubation, all compounds showed equal activity. This supports the postulate that biological activity may depend more on the total concentration of vanadium than on the form in which it was used [95]. It was also shown that, regardless of the oxidation state in model vanadium (V), (IV) and (III) compounds, including vanadate and BMOV, after a 24-hour incubation in the cell culture medium, approximately 75% of the total vanadium was vanadium(V). Similarly, vanadium speciation in HepG2 hepatocytes also varied with incubation time, with vanadium(IV) accounting for ~20% to ~70% of the total vanadium pool, largely independent of the vanadium complex used or the dominant vanadium oxidation state in the medium [96].

Prolonged incubation of the cells with vanadium complexes, as it did during the study of the effect on glucose consumption, more closely corresponds to the actual conditions of clinical use, also allowing for the identification of possible cytotoxic effects. These effects were not observed, as cell viability was not lower than 80% of the vehicle control for all tested complexes. This level is interpreted as a lack of cytotoxic effect according to the ISO rules for in vitro cytotoxicity tests [56]. For some complexes, an increase in the signal in the viability assay was observed, which may be due to the metabolic activation of the cells. A Resazurin-based reagent is reduced proportionally to metabolic activity of cells as a result of the transference of electrons from  $\text{NADPH} + \text{H}^+$ , the amount of which strictly depends on glucose metabolism [98]. Similar results for vanadium complexes have already been observed using C2C12 myocytes and the MTT test based on the same mechanism [98].

In this study, among the ONS complexes, only VC070 enhanced the transport of [14C]-deoxy-D-glucose in both models. The rest of complexes in this group did not demonstrate significant activity in 3T3-L1 adipocytes; however, their activity on myocytes was significant. This activity was higher than the activity of BMOV and  $\text{VOSO}_4$ , although clearly lower than the activity of ONO complexes.

VC070 differed from the other complexes of this group only in its starting amino acid, which was leucine. It can be assumed that this complex interacts with the amino acid transporter SLC7A5 (LAT1), which is the main leucine transporter in the body. It is also a



transporter with broad substrate specificity, capable of transporting large hydrophobic neutral amino acids as well as many drugs [99, 100]. Structural analogues of leucine and leucine-related compounds can also be transported by SLC7A5. The involvement of this transporter in the cellular transport of ruthenium complexes has also been suggested [101]. It is possible that in the body the donor complexes of ONS may be degraded and release the amino and carboxyl groups of the starting amino acids. On the other hand, other amino acids that were the starting amino acids in our ONS complexes can also be transported using this transporter. These complexes showed activity in myocytes where SLC7A5 has the highest expression and significantly lower activity in adipocytes where only VC070 with leucine as the starting amino acid was active. Differences in effect on adipocytes may be due to varying degrees of cellular amino acid uptake. The concentration of leucine in adipocytes is almost twice as high as, for example, phenylalanine or methionine, starting amino acids in other ONS complexes that did not show such a strong effect [102].

The possible synergistic effect of vanadium and the lysine derivative formed after the possible breakdown of the complex on the observed increase in glucose transport should also be considered. Leucine may enhance the transport of deoxy-D-glucose to myocytes by an insulin-independent mechanism as well as by promotion of glucose transporters translocation to the plasma membrane [103, 104].

The assumed involvement of the SLC7A5 transporter in the transport of ONS complexes to the cells could explain the lack of effect of ONS complexes on lipid accumulation in the model of non-alcoholic fatty liver disease. Oleic acid, used to induce hepatocyte steatosis, as a cis-unsaturated long-chain fatty acid, inhibits the transport of amino acids to cells [105, 106]. The concentration of BSA in the medium (0.1%) may have been insufficient to bind free oleic acid and eliminate the effect on transport inhibition. This could explain why all of the tested ONS complexes showed high activity against the same hepatocytes in the gluconeogenesis inhibition experiment in which the cell medium did not contain oleic acid.

We undertook research on the hepatic effects of the ONS and ONO complexes because systemic metabolic disorders such as diabetes and obesity are closely related to the dysfunction of the liver as the central organ that maintains metabolic homeostasis. We conducted research in the model of non-alcoholic fatty liver disease (NAFLD), which is a continuum of liver dysfunction caused largely by dietary and lifestyle factors. Hepatocyte steatosis is often observed in insulin resistance and diabetes, and NAFLD itself, as it progresses, often leads to cirrhosis and hepatocellular carcinoma [107]. NAFLD is characterized by excessive storage of lipids in the cytosol of hepatocytes with impaired function, which is accompanied by a number of changes in the course of glucose and lipid metabolism and insulin resistance. These processes are of systemic importance in diabetes and obesity.

As mentioned above, the ONS complexes showed no reduction in lipid accumulation, while the two ONO complexes, VC067 and VC068, were found to be very active in inhibiting intracellular lipid accumulation. The lack of cytotoxic effects with reduction in cell number indicates that the observed effect was not due to the reduction in cell number.

In the studies of other authors, similar effects were shown for vanadium(IV)-chlorodipicolinate in primary rat hepatocytes and hepatocytes HepG2 treated with palmitate. A significant decrease of the intracellular lipid contents in a dose-dependent manner ranging from 50-200  $\mu$ M was observed. An analogous effect for this complex was also observed in liver tissue from mice fed a high-fat diet [108]. Most of the few studies on the effect of vanadium complexes on liver lipid disturbances used in vivo models and demonstrated effectiveness against the mechanisms responsible for fatty liver [109, 110].

For some ONO complexes, we observed an increase in lipid accumulation in hepatocytes. Several possible causes must be considered in explaining this effect. This may indicate hepatotoxicity consistent with drug-induced steatohepatitis (DISH), which is a form of drug-induced liver injury (DILI) caused by various drugs [57]. In cell models, this can



manifest as lipid accumulation without significant damage to cell membranes or cell death. The observed effects may be related to the presence of phenanthroline as a co-ligand, which may increase the cytotoxicity of vanadium complexes [111]. In the studies, the oxidation of V(IV) to V(V) was observed with the release of phenanthroline ligand, which in its free form was responsible for most of the observed cytotoxic effects [112]. Free phenanthroline is able to complex iron ions, facilitating its transport into the cell. This may intensify oxidative stress, which is an important mechanism of hepatocyte steatosis. Vanadium compounds may have a pro-oxidative effect, depending on the degree of oxidation or the presence of other ligands, which may lead to lipid peroxidation in the liver [113, 114].

Although metabolic processes aim to eliminate xenobiotics from the body as quickly as possible, they can transform non-toxic compounds into reactive metabolites at various stages. The structure of compounds can have sites or groups that are more susceptible to metabolic bioactivation, which can result in metabolites of varying chemical reactivity and thus varying degrees of toxicity [115].

Halogenated aromatic hydrocarbons, such as those studied ONO complexes with bromo moieties in the aromatic rings, undergo biodehalogenation. This process can generate particularly reactive intermediate metabolites. They can bind to nucleophilic sites in biological macromolecules, leading to their modification and cytotoxic and genotoxic effects [115, 116]. In the case of the ONS complexes, the formation of chlorinated organic derivatives during their degradation is unlikely, as such structures are not components of the complexes and were not used in their synthesis.

The use of halogens in medicinal chemistry is becoming increasingly common due to their modulatory effects, and 14 out of the 50 molecules approved by the FDA in 2021 contain halogens [117]. The halogen substituent affects potency, inhibitory activity or binding affinity as well as having a pronounced effect on pharmacokinetic parameters and may determine cytotoxic effects. For example, in vitro cytotoxicity studies conducted on the human cancer cell line T47D have shown that the parent indole compound, which was essentially inactive, became the most active compound in the series when two hydrogen atoms on different rings were substituted with chlorine atoms. The modified compound exhibited over a 2500-fold improvement in cytotoxic potency [118].

Chloro-substitution is also employed in the synthesis of enhanced vanadium complexes, and the vanadium complexes with chloro-substituted Schiff base ligands exhibited increased hydrophobicity, hydrolytic stability, and ease of reduction compared to their non-chlorinated counterparts. These vanadium(V) complexes with substituted catecholates as co-ligands demonstrated potent in vitro anticancer activity [119]. On the other hand, the effects of the presence of halogens in the aromatic ring may not be unambiguous. Vanadium(IV)-chlorodipicolinate with a chlorine ligand at position 4 in the pyridine ring of dipicolinic acid showed beneficial effects in a mouse model of non-alcoholic fatty liver disease (NAFLD), effectively preventing hepatic steatosis and also mitigating oxidative stress and endoplasmic reticulum (ER) stress [109].

In our study, no certain and significant cytotoxic effects were observed. However, various reactions can occur in the metabolism of xenobiotics, and the intermediate and final metabolites can be difficult to predict. For our complexes, as with any drug candidate, the metabolic stability and toxicity of metabolites are important issues that should be considered in extended studies, especially in the later stages of preclinical development (hit-to-lead and lead optimization) [118].

The accumulation of lipids in hepatocytes observed under the influence of some ONO complexes may also result from the stimulation of glucose transport and the intensification of lipid synthesis in the hepatocytes.

All of the tested ONS and ONO complexes showed an effect on the gluconeogenesis process, inhibiting glucose synthesis in hepatocytes. Most of the studies on the effect of vanadium on gluconeogenesis come from earlier studies in animal models, and only a few studies deal with vanadium in the form of complexes [120-123]. All these studies confirm

that the antidiabetic effect of vanadium is also manifested in the inhibition of hepatic gluconeogenesis, which is an important mechanism of glucose metabolism disorders and an effective therapeutic target [124]. Vanadium inhibits gluconeogenesis by inhibiting the expression of key genes that control this process: phosphoenolpyruvate carboxykinase (PEPCK) and glucose 6-phosphatase (G-6-Pase). This is done through activation of AKT kinases with an enhanced phosphorylation of GSK-3 and FOXO, the main transcription factor of these genes [125].

Phosphorylation of AKT kinases has also been implicated as the primary mechanism of the antidiabetic action of vanadium compounds [126]. In this study, we have demonstrated that both ONS and ONO complexes potentiate the phosphorylation of AKT in hepatocytes. This indicates that they act through the same, shared mechanism, which is also the effector mechanism of insulin action. Abnormalities in the phosphorylation of AKT kinases are associated with the occurrence of insulin resistance in cells, and restoring their sensitivity to insulin is a key aspect of the pharmacotherapy of metabolic disorders. The insulin resistance of hepatocytes is caused, among other things, by exposure to increased concentrations of free fatty acids and hyperinsulinemia, and pro-inflammatory cytokines, such as TNF, intensify this process [127]. These factors were used to induce insulin resistance in the models used in this study.

The ONO complexes VC067 and VC068, which showed effects in both inhibiting lipid accumulation in the NAFLD model and inhibiting gluconeogenesis, can also reverse the effects of insulin resistance in hepatocytes. The few studies conducted in cellular models of hepatocytes have shown similar effects. Vanadium effectively reversed hepatocyte insulin resistance, induced by TNF [128], and the VO-OHPic vanadium complex's mechanism of reversing insulin resistance was related to the inhibition of the dual specificity phosphatase, PTEN. Vanadium is an inhibitor of this phosphatase that regulates the activity of the AKT pathway [129].

Normal insulin signaling networks employ not only AKT but also extracellular signal-regulated kinase (ERK). ERK has been implicated in the development of insulin resistance associated with obesity and type 2 diabetes mellitus. ERK is also the final effector of the pathway regulating the cell cycle and cell differentiation, and abnormal, uncontrolled activation is associated with neoplastic processes. In our study, all of the tested ONS and ONO complexes showed enhanced ERK phosphorylation. Dose- and time-dependent activation of the ERK signaling pathway through its phosphorylation was also found for vanadium compounds, which was associated with their anticancer effect. ERK activation through the PI3-K and ras pathway is also hypothesized to play an essential role in mediating the insulin-mimetic effects of vanadium compounds [22].

The observed differences in the effectiveness of ONS and ONO complexes in the different cell models and mechanisms may be due to the specific or selective effects of these complexes. Differences in the activity of vanadium complexes on various cell types have already been observed for bis-coordinated oxidovanadium(IV) complexes with the imidazolyl-carboxylate moiety which improved glucose uptake in cell cultures of myocytes C2C12, adipocytes 3T3-L1, and Chang cells [73]. For example,  $[\text{VO}(\text{Im}_2\text{COO})_2]$  showed efficacy on 3T3-L1 adipocytes with no activity on C2C12 myocytes.  $[\text{VO}(\text{Im}_4\text{COO})_2]$  showed the opposite effect and even decreased basal glucose utilization for 3T3-L1. Similar differences have also been observed for hepatocytes. Explaining the differences in the observed effects, the authors of this paper point to the potential possibility of structural rearrangement or decomposition of complexes, which were incubated with cells in two different media (DMEM or RPMI-1640, 10% FBS). On the other hand, two different cell models (myocytes C2C12 and Chang cells) were maintained in the same medium (RPMI-1640), yet differences in the effects of the complexes were observed. This indicates their selective action resulting from the structure of the complexes [73].

The selectivity of the effects of vanadium complexes against different cell lines cultured and incubated under the same experimental conditions has already been observed, among other things, for vanadium complexes with orotic and glutamic acids [130].

Similarly, structural modifications of the ligands of other complexes resulted in selectivity between cancer cell lines [101].

Among the possible reasons for the different intensity of the effects of vanadium complexes in different cell types is the interaction of the properties of the cells themselves and the physicochemical properties of the complexes. Preferential uptake of vanadium(V) complexes with hydrophobic organic ligands by cancer cells has been observed [131]. Such interactions may result from the different composition, structure and properties of cell membranes in different tissues and specific changes in membranes in cancer cells [132]. Differences in these properties naturally also concern normal cells from various tissues. An example illustrating the influence of cell properties on interactions with vanadium complexes may be the degree of cell differentiation of 3T3-L1 adipocytes. The differentiation of these cells from preadipocytes to adipocytes is accompanied by changes in the amount and composition of intracellular lipids. 3T3-L1 mature adipocytes, as compared to preadipocytes of this cell line, showed a greater tendency to form vanadium IV, despite the predominance of form V in the medium [96]. Similarly, steatotic hepatocytes are characterized by altered biochemical processes and structural differences from normal hepatocytes, which include, among other things, modifications of cell membranes. This may determine the specific effects and activity of the ONS and ONO complexes.

#### 4. Conclusions

In this study, we confirmed that the novel synthesized and characterized ONS-type vanadium(V) complexes with thioanilide derivatives of amino acids show pharmacological activity in the cell models of metabolic disturbances.

Our research approach with a wide range of models and investigated mechanisms, adequate to the wide range of activity of vanadium complexes, allowed for the identification of complexes that specifically act on myocytes, adipocytes and hepatocytes as well as the pathogenetic processes of metabolic disorders, including NAFLD.

The ONS complexes have shown inhibition of human protein tyrosine phosphatases (PTP1B, LAR, SHP1 and SHP2) in the submicromolar range ( $IC_{50}$  in the range of 13 – 141 nM), as well as inhibition of non-tyrosine phosphatases (CDC25A and PPA2), similar to bis(maltolato)oxovanadium(IV)(BMOV). The ONO complexes showed weaker inhibition than ONS complexes ( $IC_{50}$  in the range 0,23 – 4,26  $\mu$ M).

The simultaneous testing of ONO-type complexes made possible a direct comparison of the potential and strength of action between the two groups of complexes. In addition to the differences in the pharmacological effects of the ONS and ONO group complexes, within each of these groups, we identified complexes with effects that distinguished them from other complexes in the same group. VC070, as the only ONS type complex that enhanced transport of [14C]-deoxy-D-glucose in C2C12 myocytes and 3T3-L1 adipocytes (158 $\pm$ 10% and 159 $\pm$ 14% of the control, respectively). In contrast, the ONO-type complex VC032 caused an increase of this transport into myocytes (266 $\pm$ 36% of control) and no effect in adipocytes (97 $\pm$ 14%).

VC068, from the ONO group complexes, showed high activity in all of the employed cell models. For example, this complex at a concentration of 50  $\mu$ M increased transport of [14C]-deoxy-D-glucose in C2C12 myocytes (218 $\pm$ 10%) and 3T3-L1 adipocytes (177 $\pm$ 3% of the control). Moreover, VC068 inhibited gluconeogenesis in hepatocytes HepG2 by 79 $\pm$ 18%, and decreased lipid accumulation in the non-alcoholic fatty liver disease model using the same cells by 36 $\pm$ 7% (relative to controls).

Our study serves as the basis for further research on the selective or specific effects of vanadium complexes, which may help develop vanadium complexes with improved pharmacological properties.

## 5. Materials and Methods

### 5.1. Complexes synthesis and characterization

#### 5.1.1. Materials and analytical methods

All reagents were of analytical grade (Aldrich) and were used as supplied. Ethanol (98%) was of pharmaceutical grade and all other solvents were of analytical grade and were used as supplied.

Microanalysis of carbon, hydrogen and nitrogen and sulfur were performed using Elementar Vario MICRO Cube elemental analyzer. The IR spectra for ligands L1-L5 were recorded using a Nicolet iSS FT-IR spectrophotometer, while those for the complexes were recorded using a Bruker EQUINOX 55 FT-IR spectrophotometer in KBr pellets. The electronic absorption spectra were recorded with Shimadzu UV-3600 UV-Vis-NIR spectrophotometer equipped with a CPS-240 temperature controller. The magnetic susceptibility measurements were performed on a SHERWOOD SCIENTIFIC magnetic susceptibility balance. NMR spectra were determined on a Bruker Avance II 300 MHz spectrometer (using TMS as an internal standard).

#### 5.1.2. The synthesis of vanadium complexes with ONS Schiff base ligands

##### 5.1.2.1. Synthesis of 3-hydroxythioprotonic acid anilide

Stage 1 (Scheme 1 in the section *Results*): A solution of acetylacetone (acac) (40.1 g; 41.2 mL, 0.4 mol) in anhydrous DMF (150 mL) was cooled to 0 °C by immersing the reaction flask in ice water. Separately, sodium hydride NaH, without of paraffin oil, was prepared according to the following procedure: commercial NaH dispersed in paraffin oil (55%-60%) was placed in a column with a glass filter, connected to a water pump, and washed with small portions of anhydrous diethyl ether (3 × 10 mL) thus removing the paraffin oil. Pure 100% NaH was dried by passing a stream of argon through the column, still connected to the water pump. Oil free NaH (9.6 g; 0.4 mol) was added gradually to a cooled acac solution in DMF. During the addition of NaH, hydrogen was rapidly evolved and then the contents of the flask solidified to a white mass, which was broken with a baguette. After 1 hour phenyl isothiocyanate PhNCS (54.1 g; 51.2 mL; 0.4 mol) was added dropwise while stirring the contents of the flask with a magnetic or mechanical stirrer. The reaction mixture turned brown red color. After one hour of stirring, the solution was poured onto 500 g of ice and acidified with HCl (1:1) to pH = 6. A brown oil precipitated solidified over time and turned yellow. It was a 2-acetyl derivative of 3-hydroxythioprotonic acid anilide.

Stage 2 (Scheme 1 in the section *Results*): 3.41 g of sodium hydroxide and 65 mL of distilled water were introduced into a 250 mL beaker. The beaker was placed on a magnetic stirrer and its content was heated to 60 °C, then 20 g of 2-acetyl-3-hydroxythioprotonic acid anilide were dissolved in the contents of the beaker with vigorous stirring. The resulting solution was left in an ice bath for several hours. The resulting light yellow precipitate of 3-hydroxythioprotonic acid anilide was filtered off. The precipitate was crystallized from benzene, giving the product in the form of yellow flakes, m.p. 63-65 °C (lit. 64-66 °C). The yield after crystallization is 11.97 g (73%) of product III (Scheme 1). The product can also be crystallized from ethanol, but the crystallization efficiency is lower and does not exceed 55%.

##### 5.1.2.2. Condensation reaction of 3-hydroxythioprotonic acid anilide with an amino acid salt

Condensation reaction is illustrated in Scheme 2 in the section *Results*. 3-Hydroxythioprotonic acid anilide (5.336 g; 27.61 mmol) was added to a 100 mL round bottom flask, which was dissolved in benzene (65 mL). Then a small amount of DMF (1 mL) and the sodium salt of the amino acid (26.77 mmol) were triturated in a mortar. As amino acid we

used L-tryptophan, L-phenylalanine, L-leucine, L-methionine, D/L-isoleucine. The flask was placed on a magnetic stirrer in an oil bath and an azeotropic head and reflux condenser were attached. The reaction mixture was heated 4-14 hours to reflux - the oil bath temperature was 120 °C, until no more water separation was obtained. The formed yellowish precipitate IV (Scheme 2) was filtered after cooling, washed with toluene, then with petroleum ether and dried. In formulas of vanadium complexes with ONS ligands, the compound IV is marking as L<sub>1</sub> to L<sub>5</sub> (for R = L-tryptophan, L-phenylalanine, L-leucine or L-methionine, D/L-isoleucine, respectively).

#### 5.1.2.3. Syntheses of complexes with ONS ligands (VC054, VC059, VC070, VC073, VC109)

The synthesis of complexes with the ONS ligands is illustrated in Scheme 3 in the *Results* section. For a suspension of IV (3 mmol) in anhydrous THF (25 mL) 2 M HCl in diethyl ether (Et<sub>2</sub>O) (3 mmol; 1.5 mL) was added dropwise. The mixture was practically clarified during the addition of HCl in Et<sub>2</sub>O. 30 min after the end of the addition of HCl in Et<sub>2</sub>O, VOCl<sub>3</sub> (3 mmol; 0.52 g; 0.28 mL) was added dropwise. The color of the mixture changed from yellow to dark green during the addition of VOCl<sub>3</sub>. 30 min after the end of the VOCl<sub>3</sub> addition, the contents were centrifuged (4000 min<sup>-1</sup>, 4 min) and the supernatant was evaporated on a rotary evaporator (60 °C). The green-brown (olive) residue was dried in a vacuum oven (60 °C, 4 h). In the Table 1 in the section *Results* the formulas of ligand and complexes with the elemental analysis and IR spectra results are given.

#### 5.1.3. The synthesis of vanadium complexes with ONO Schiff base ligands

The syntheses of selected ONO complexes were previously described in [45-47].

##### 5.1.3.1. Synthesis of ONO complex [V(L<sub>13</sub>)(HL<sub>13</sub>)] (VC055)

The 5-bromosalicylaldehyde (0.603 g, 3.0 mmol), 4-methoxybenzhydrazide (0.496 g, 3.0 mmol) and EtOH (20 mL) were refluxed under Ar for 15 minutes. Then [V(acac)<sub>3</sub>] (0.528 g, 1.5 mmol) was added and reflux was continued for 20 minutes. Almost immediately formation of brown precipitation was observed and solution started to be light yellow. The mixture was cooled and filtered and the complex was washed three times with excess of EtOH and dried in air. Yield: 0.936 g, 84%. MW = 746.27. Anal. Calcd. for C<sub>30</sub>H<sub>23</sub>Br<sub>2</sub>N<sub>4</sub>O<sub>6</sub>V: C, 48.28; H, 3.11; N, 7.51 %. Found: C, 48.03; H, 3.71; N, 6.94 %. The complex is paramagnetic,  $\mu = 1.50 \mu_B$ . IR-ATR (cm<sup>-1</sup>): 3456 (w), 2956 (w), 1607 (s), 1509 (m), 1489 (w), 1456 (w), 1412 (w), 1365 (m), 1338 (w), 1308 (w), 1258 (m), 1177 (m), 1137 (w), 1087 (w), 1030 (m), 936 (w), 902 (w), 872 (w), 845 (w), 822 (w), 756 (w), 701 (w), 657 (w), 620 (w), 579 (w), 469 (w).

#### 5.2. Methods of biological assays

##### 5.2.1. Materials

Molecular biology grade or pure for analyzes reagents were used for biochemical assays. Media and consumables of appropriate quality and purpose were used for cell cultures were obtained from American Type Culture Collection (ATCC), Lonza, Thermo Fisher Scientific and Sigma-Aldrich.

##### 5.2.2. Inhibition of human recombinant tyrosine phosphatases

To determine the ability of tested compounds to inhibition tyrosine phosphatases [46, 128], human recombinant proteins were used (Sigma-Aldrich, USA). The reactions were performed in black opaque 384-well microplates (PerkinElmer, USA). An equal volume of phosphatase solution in a reaction buffer (25 mM of 3-(N-morpholino)propanesulfonic acid (MOPS), 50 mM NaCl, 1 mM dithiothreitol (DTT) and 0.05% Tween-20, pH 7.0) was added to the solution of the tested compound on microplate. These solutions were dispensed using automated injector. The following final concentrations of the tested



phosphatases were used: PTP1B 50 ng/mL, SHP1 400 ng/mL, SHP2 50 ng/mL, LAR 5 ng/mL and PTPRA 100 ng/mL. After 10 min, a solution of phosphate 6,8-difluoro-4-methyl (DiFMUP; Thermo Fisher Scientific, USA) was added until its final concentration was 0.1 mM. Samples were incubated for 20 minutes at 23 °C and then the measurements of fluorescence intensity (excitation 355 and emission 560 nm) were performed on a multifunctional plate reader POLARstar Omega (BMG Labtech, Germany). Assays were performed in triplicates. For the screening assays the final concentration of tested compounds was 1 µM. The results were expressed as per cent of inhibition of untreated control (enzyme with vehicle only) for the screening tests. For determination of the half maximal inhibitory concentration (IC<sub>50</sub>) nine concentrations of tested compound in the range 10 nM to 10 µM was assayed in triplicates. IC<sub>50</sub> were calculated using GraphPad Prism version 6.0 software (GraphPad Software, USA).

#### 5.2.3. Inhibition of human recombinant non-tyrosine phosphatases

For inhibition assay of non-tyrosine phosphatases [129], human recombinant protein were used (Sigma-Aldrich, USA). The reactions were performed in black opaque 384-well microplates (PerkinElmer, USA). To the solution of the tested complexes an equal volume of a test solution of phosphatase was added. CDC25A were diluted in reaction buffer to the final concentration 400 ng/mL as for tyrosine phosphatases (described in the section above), and PPA2 (final 0.5 U/mL) was diluted in 50 mM Tris-HCl, 0.05% Tween-20, 125 µg/mL protease free bovine serum albumin, pH 7.0. These solutions were dispensed using automated injector. After 10 minutes, a solution of phosphate 6,8-difluoro-4-methyl (DiFMUP; Thermo Fisher Scientific, USA) was added for PPA2 sample until for the final concentration 0.1 mM. For CDC25A samples 3-O-methylfluorescein phosphate for the final concentration 0.2 mM was added. Samples were incubated for 180 minutes at 23 °C and then the measurements of fluorescence intensity (excitation 355 and emission 560 nm) were performed on a multifunctional plate reader POLARstar Omega (BMG Labtech, Germany). Assays were performed in triplicates. The results were expressed as per cent of inhibition of untreated control (enzyme with vehicle solvent only).

#### 5.2.4. Cell models and culture conditions

All cell lines were obtained directly from ATCC (American Type Culture Collection). The passage number of cells used in the experiments was between 4 and 10. The evaluation of the functional stability of the cell lines was conducted based on the results for control compounds, which were tested in each experimental series and compared with the results obtained in the process of validation and optimization of experimental models.

Myocytes C2C12 cell line (ATCC CRL-1772), subclone of myoblasts from mouse muscles were cultured according to standard protocol in DMEM supplemented with 10% fetal calf serum, 100 IU/ml penicillin and 100 mg/ml streptomycin at 37 °C in 5% CO<sub>2</sub>. Cells were plated on 96-well microplate and after reach confluence were differentiated in medium with 2% horse serum. Differentiation medium was changed every 72 h.

Adipocytes 3T3-L1 cell line (ATCC CRL-11605) derived from fibroblasts from mouse embryo tissue were cultured according to standard protocol in DMEM medium supplemented with 10% bovine calf serum, 100 IU/mL penicillin and 100 mg/mL streptomycin at 37 °C in 5% CO<sub>2</sub>. Cells were seeded in 96-well poly-D-lysine coated plates and cultured to reach confluency. The culture medium was then replaced for differentiation medium I (DMEM, 10% foetal bovine serum, 25 nM 3-isobutyl-1-methylxanthine (IBMX), 500 µM dexamethasone, and 670 nM/10 µg/mL human recombinant insulin). After 48 hours of incubation (differentiation day 2), the medium was changed to differentiation medium II (DMEM, 10% foetal bovine serum, and 670 nM/10 µg/ml human recombinant insulin).

Human hepatocytes HepG2 cell line (ATCC HB-8065) were cultured according to standard protocol in DMEM supplemented with 10% fetal bovine serum, 100 IU/mL



penicillin and 100 mg/mL streptomycin at 37 °C in 5% CO<sub>2</sub>. Cells were plated on 96-well microplate and use 18-24 h after seeding.

#### 5.2.5. Scintillation proximity assay for uptake of radiolabeled 2-deoxy-D-[U-14C]-glucose

Scintillation proximity assay (SPA) is a method to measure real time accumulation of radiolabeled substrates by adherent cells with no filtration needed. Radioactivity concentrated closer to the scintillator embedded in the plastic bottom of each well provides a stronger signal than the radiolabeled substrate in the culture medium [130]. Uptake of radiolabeled 2-deoxy-D-[U-14C]-glucose was conducted based on previously descriptions [131-133].

Hepatocytes HepG2, myocytes C2C12 (after 8 days differentiation) and adipocytes 3T3-L1 (after 11 days of differentiation) was cultured and maintained as described in section above but plated on ScintiPlate TC 96-well microplate coated with solid phase scintillator (PerkinElmer, USA). Hepatocytes and myocytes were washed and culture medium was changed for medium with 0.5% BSA instead serum. After 24 h incubation tested complexes were added. After 2 h incubation at 37 °C in 5% CO<sub>2</sub> medium was changed for low glucose medium (1000 mg/l), tested complexes were added again and further incubation for 4 h was conducted. Next, cells were washed three times with Krebs-Ringer buffer (KRB) without glucose (1 mM MgSO<sub>4</sub>, 1 mM CaCl<sub>2</sub>, 136 mM NaCl, 4.7 mM KCl and 10 mM HEPES; pH 7.4) and KRB with human recombinant insulin at final concentration 100 nM (Sigma-Aldrich) was added for 15 min. Wortmannin at final concentration 200 nM (Sigma-Aldrich) was used as negative control. After that, cells were washed three times with cold KRB and cytochalasin B (10 mM final) was added for several wells as “no uptake” control and proceeded as shown below.

Adipocytes were washed and medium was changed for basal medium. After 24 h incubation tested complexes were added. After 2 h incubation at 37 °C in 5% CO<sub>2</sub> medium was changed for DMEM medium without glucose, with 0.1% BSA free from fatty acid, 200 mM L-glutamine and 100 mM pyruvate. Tested complexes were added again and further incubation for 4 h was conducted. Next, cells were washed three times with Krebs-Ringer buffer (KRB) without glucose and KRB with human recombinant insulin at final concentration 100 nM (Sigma-Aldrich) was added for 15 min. Wortmannin at final concentration 200 nM (Sigma-Aldrich) was used as negative control. After that, cells were washed three times with cold KRB and cytochalasin B (10 mM final) was added for several wells as “no uptake”.

For cells proceeded as above 2-deoxy-D-[U-14C]-glucose (250-350 mCi/mmol, NEC720A, PerkinElmer, USA) solution in KRB with total activity 0.03 mCi was added to each well. After 1 h incubation at 37 °C and 5% CO<sub>2</sub> uptake was blocked by adding cytochalasin B (10 mM final). Radioactivity of samples was measured in scintillation counter MicroBeta Trilux 1450 (PerkinElmer, USA). Non-specific radioactivity was subtracted from each result (cpm). Two independent experiments with triplicates were conducted. Final results were expressed as per cent of control contained solvent only instead tested compound.

#### 5.2.6. Glucose utilization in myocytes

Differentiated myocytes C2C12 was used after 8 days differentiation. The culture medium was changed for medium with 0.2% bovine serum albumin, 100 IU/mL penicillin, 100 µg/mL streptomycin and after 2 hours incubation the medium was changed for fresh medium containing tested compounds. After 24 hours incubation, supernatants were collected.

Glucose concentration was determined based on enzymatic reaction with glucose oxidase and fluorometrically detection reaction end product using AmplexRed Glucose/Glucose Oxidase Kit (Invitrogen) according to manufacturer protocol. 10 mL supernatant diluted 50x in 50 mM PBS pH 7.4 and 10 mL reagents containing 4 U/mL glucose

oxidase, 0.4 U/mL horseradish peroxidase and 200 mM 10-acetyl-3,7-dihydroxyphenoxazine in 50 mM PBS pH 7.4 was added to a black opaque 384-well OptiPlate and incubated for 30 minutes at 37 °C. All assays were conducted in triplicates. Fluorescence signal was measured at excitation of 530 nm and emission of 580 nm using a multimodal microplate reader POLARStar Omega (BMG Labtech, Germany) and glucose concentration in samples was calculated in MARS Data Analysis Software based on glucose standards. Glucose utilization was calculated as the differences between incubation medium without cells and medium with cells after incubation with the tested compound. Final results were expressed as the per cent of controls containing cells and solvent only.

#### 5.2.7. Inhibition of lipid accumulation in cell model of NAFLD

Induction of hepatic lipid accumulation and studies on the effect of vanadium complexes on this process were carried out based on previous descriptions [134, 135]. Hepatocytes HepG2 in culture medium (as indicated above) were seeded on collagen-I coated 96 well microplate in amount of 20,000 per well. After 16-24 hour standard medium was changed for DMEM with 0.1% BSA fatty acid free and 0.5 mM oleic acid as sodium salt and tested compounds were added. Cells were incubated for 24 h and the intracellular lipid content was evaluated using AdipoRed Adipogenesis Assay Reagent (Lonza, Switzerland) according to the manufacturer's protocol. Hepatocytes were washed with PBS with calcium and magnesium and 5 µL AdipoRed Reagent in 200 µL PBS was added and incubated for 10 minutes in 22 °C. Fluorescence signal proportional to lipids content in cells was measured at excitation in 530 nm and emission in 550 nm using multimodal microplate reader POLARStar Omega (BMG Labtech, Germany). The results were normalized to the untreated control (cells with solvent only), wherein the intensity of fluorescence was taken as 100%.

#### 5.2.8. Inhibition of hepatic gluconeogenesis

Experiments on inhibition of hepatic gluconeogenesis in HepG2 hepatocytes by the vanadium complexes were carried out based on previous description with some modifications [136]. Hepatocytes HepG2 in culture medium (as indicated above) were seeded on half-area 96 microplate in amount of 50,000 per well. After 16-24 h cells were washed with PBS three times and one time with experimental medium (DMEM without glucose with 0.1% BSA, 2 µM L-glutamine, 15 mM HEPES, 1 mM sodium pyruvate, 10 mM calcium lactate, 100 IU/mL penicillin and 100 mg/mL streptomycin). Cells were incubated in this medium for 3 h at 37 °C in 5% CO<sub>2</sub> and next medium was changed for experimental medium with additional gluconeogenesis inducers: 10 µM dexamethasone, 100 µM 8-bromoadenosine 3',5'-cyclic monophosphate sodium salt (8-Br-cAMP) and 500 µM 3-isobutyl-1-methylxanthine (IBMX). After adding test compounds the cells were incubated for 3 h at 37 °C in 5% CO<sub>2</sub> microplate and supernatant was collected for glucose assay (as described in section "Glucose utilization in myocytes"). Glucose synthesis was calculated as glucose concentration differences between experimental medium without cells and medium with cells after incubation with the tested compound. Final results were expressed as per cent of inhibition of glucose synthesis by cells incubated with solvent only.

#### 5.2.9. Hyperinsulinemia condition and induction of insulin resistant hepatocytes

Induction of insulin resistant hepatocytes HepG2 were carried out based on previous descriptions [137, 138]. Hepatocytes HepG2 in culture medium (as described in section above) were plated on ScintiPlate TC 96-well microplate coated with solid phase scintillator (PerkinElmer, USA). After 16-24 h medium was changed for medium with addition of human recombinant insulin at concentration 10 µg/mL or with insulin resistant inducers: 10 ng/mL TNF-α or oleic acid as sodium salt and cells were incubated for next 48 h at 37 °C in 5% CO<sub>2</sub>. Next, compounds in fresh medium were added and further incubation

was carried out for 24 h and scintillation proximity assay for uptake of radiolabeled 2-deoxy-D-[U-<sup>14</sup>C]-glucose was conducted as described in section above.

#### 5.2.10. Cytotoxicity assay (cell membrane damage)

The bioluminescent ToxiLight assay (Lonza) was used as a highly sensitive cytotoxicity assay designed to measure cell membrane damage [139]. After incubation of cells with the tested compounds, 10 µL of cell supernatant was deposited in a new 96-well plate. Then, 40 µL of the Adenylate Kinase Detection Reagent (AKDR) was added per well. After 5 minutes of incubation at 22 °C, the luminescence intensity was measured in a multifunction plate reader (POLARstar Omega, BMG Labtech). The results were expressed as per cent of signal of untreated control (cells with solvent only).

#### 5.2.11. Homogeneous proximity-based assay for AKT and MAPK/ERK phosphorylation

Hepatocytes HepG2 were seeded on 96-well microplate and incubated in culture medium without serum for 3 h and next were washed three times with Krebs-Ringer buffer (KRB) (NaCl 115 mM NaCl, 4.7 mM KCl, 1.28 mM CaCl<sub>2</sub>, 1.2 mM MgSO<sub>4</sub>, 1.2 mM KH<sub>2</sub>PO<sub>4</sub>, 10 mM NaHCO<sub>3</sub> 25 mM HEPES, pH 7.4). Tested compounds were added in serum-free culture medium and cells were incubated for 30 minutes for AKT and 20 minutes for ERK assay at 37 °C in 5% CO<sub>2</sub> medium. Next, cells were washed, incubated for further 1 and 3 h and washed again before assay.

Protein phosphorylation was assayed using homogenous proximity-assay [140] with AlphaScreen SureFire Akt 1/2/3 (p-Ser473) Assay Kit and AlphaScreen SureFire ERK 1/2 (p-Thr202/Tyr204) Assay Kit (PerkinElmer, USA) according to manufacturer's manual. Cells were lysed with Lysis Buffer with shaking for 10 minutes (350 rpm). 30 µL of the lysate was transferred to the white opaque 96 well half-area assay plate and 10 µL Acceptor Mix was added. Microplate was agitated on plate shaker for 2 minutes (350 rpm), and then incubated for 2 hours at 23 °C. 10 µL of Donor Mix was added to the wells under subdued light and microplate was agitated on plate shaker for 2 minutes (350 rpm), and then incubate for 1 hour (Akt) or 3 h (ERK) at 23 °C in darkness. Alpha signal was measured in standard mode using multimodal microplate reader POLARStar Omega (BMG Labtech, Germany). The results were expressed as ratio of phosphorylated protein to total protein and normalized to the untreated control (cells with solvent only), wherein the intensity of signal was taken as 100%.

#### 5.3. Statistical methods

Unless otherwise indicated in the text, all results statistical analysis was performed by analysis of variance followed by the Dunnett test for post hoc comparisons with  $p < 0.05$ . All tests were performed using GraphPad Prism version 6.0 for Windows, (GraphPad Software, USA).

**Supplementary Materials:** The following supporting information can be downloaded at the website of this paper posted on Preprints.org, Figure S1: <sup>1</sup>H-NMR spectrum of L<sub>1</sub>; Figure S2: <sup>13</sup>C-NMR spectrum of L<sub>1</sub>; Figure S3: <sup>1</sup>H-NMR spectrum of L<sub>2</sub>; Figure S4: <sup>13</sup>C-NMR spectrum of L<sub>2</sub>; Figure S5: <sup>1</sup>H-NMR spectrum of L<sub>3</sub>; Figure S6: <sup>13</sup>C-NMR spectrum of L<sub>3</sub>; Figure S7: <sup>1</sup>H-NMR spectrum of L<sub>4</sub>; Figure S8: <sup>13</sup>C-NMR spectrum of L<sub>4</sub>; Figure S9: <sup>1</sup>H-NMR spectrum of L<sub>5</sub>; Figure S10: <sup>13</sup>C-NMR spectrum of L<sub>5</sub>; Figure S11: IR-ATR spectrum of L<sub>1</sub>; Figure S12: IR-ATR spectrum of L<sub>2</sub>; Figure S13: IR-ATR spectrum of L<sub>3</sub>; Figure S14: IR-ATR spectrum of L<sub>4</sub>; Figure S15: IR-ATR spectrum of L<sub>5</sub>; Figure S16: IR-ATR spectrum of VC054; Figure S17: IR-ATR spectrum of VC059; Figure S18: IR-ATR spectrum of VC070; Figure S19: IR-ATR spectrum of VC073; Figure S20: IR-ATR spectrum of VC109; Figure S21: IR-ATR spectrum of VC055; Figure S22: UV-Vis spectra of complex VC054 in DMSO-H<sub>2</sub>O mixture; Figure S23: UV-Vis spectra of complex VC059 in DMSO-H<sub>2</sub>O mixture; Figure S24: UV-Vis spectra of complex VC070 in DMSO-H<sub>2</sub>O mixture; Figure S25: UV-Vis spectra of complex VC073 in DMSO-H<sub>2</sub>O mixture; Figure S26: UV-Vis spectra of complex VC055 in DMSO-H<sub>2</sub>O mixture; Figure S27: Qualitative UV-Vis spectra of complex VC054 in different solvents; Figure S28: Qualitative UV-Vis spectra of complex VC059 in different solvents; Figure S29: Qualitative UV-Vis spectra of complex

VC070 in different solvents; Figure S30: Qualitative UV–Vis spectra of complex VC073 in different solvents; Figure S31: Qualitative UV–Vis spectra of complex VC109 in different solvents; Figure S32: Qualitative UV–Vis spectra of complex VC055 in different solvents.

**Author Contributions:** Conceptualization, G.K.; methodology, G.K. and D.C.; validation, G.K., M.G.-L. and B.M.; formal analysis, G.K.; investigation G.K., M.G.-L., B.M., E.M., A.J., B.T. and D.C.; resources, G.K., M.G.-L., B.M., E.M., B.T. and D.C.; data curation G.K., B.M., M.G.-L., B.T., D.C. and A.J.; writing—original draft preparation, G.K. and A.J.; writing—review and editing, M.K., M.P. and J.S.; visualization, G.K., A.J. and D.C.; supervision, G.K. and M.P.; project administration G.K.; funding acquisition G.K. and M.K. All authors have read and agreed to the published version of the manuscript.

**Funding:** This research was funded by the European Union Funds via European Regional Development Fund under the Innovative Economy Program 2007–2013, grant number WND POIG.01.03.01-174/09 and by Jagiellonian University Medical College, grant number N42/BDS/000287.

**Institutional Review Board Statement:** Not applicable.

**Informed Consent Statement:** Not applicable.

**Data Availability Statement:** The data presented in this study are available on reasonable request from the corresponding author.

**Acknowledgments:** We would like to thank Doctor Ryszard Gryboś and Professor Barbara Filipek for their invaluable contribution and support throughout the entire project.

Many thanks to the late Professor Marek Stępniewski (1939-2023), without whom this research would never have been possible.

**Conflicts of Interest:** The authors declare no conflict of interest.

## References

1. Saeedi, P.; Petersohn, I.; Salpea, P.; Malanda, B.; Karuranga, S.; Unwin, N.; Colagiuri, S.; Guariguata, L.; Motala, A.A.; Ogurtsova, K.; Shaw, J.E.; Bright, D.; Williams, R. IDF Diabetes Atlas Committee. Global and regional diabetes prevalence estimates for 2019 and projections for 2030 and 2045: Results from the International Diabetes Federation Diabetes Atlas, 9th edition. *Diabetes Res. Clin. Pract.* **2019**, *157*, 107843.
2. Grundy, S.M. Pre-diabetes, metabolic syndrome, and cardiovascular risk. *J. Am. Coll. Cardiol.* **2012**, *59*, 635-43. doi: 10.1016/j.jacc.2011.08.080
3. Lima, L.M. Prediabetes definitions and clinical outcomes. *Lancet Diabetes Endocrinol.* **2017**, *5*, 92-93. doi: 10.1016/S2213-8587(17)30011-6
4. Yip, W.C.Y.; Sequeira, I.R.; Plank, L.D.; Poppitt, S.D. Prevalence of pre-diabetes across ethnicities: a review of impaired fasting glucose (ifg) and impaired glucose tolerance (igt) for classification of dysglycaemia. *Nutrients* **2017**, *9*, 1273. doi: 10.3390/nu9111273
5. Araújo, A.R.; Rosso, N.; Bedogni, G.; Tiribelli, C.; Bellentani, S. Global epidemiology of non-alcoholic fatty liver disease/non-alcoholic steatohepatitis: What we need in the future. *Liver Int.* **2018**, *38*, 47-5. doi: 10.1111/liv.13643
6. Marjot, T.; Moolla, A.; Cobbald, J.F.; Hodson, L.; Tomlinson, J.W. Nonalcoholic fatty liver disease in adults: current concepts in etiology, outcomes, and management. *Endocr. Rev.* **2020**, *41*, bnz009. doi: 10.1210/edrv/bnz009
7. Dahlén, A.D.; Dashi, G.; Maslov, I.; Attwood, M.M.; Jonsson, J.; Trukhan, V.; Schiöth, H.B. Trends in antidiabetic drug discovery: FDA approved drugs, new drugs in clinical trials and global sales. *Front. Pharmacol.* **2022**, *12*, 807548. doi: 10.3389/fphar.2021.807548
8. Artasensi, A.; Pedretti, A.; Vistoli, G.; Fumagalli, L. Type 2 diabetes mellitus: A review of multi-target drugs. *Molecules* **2020**, *25*, 1987. doi: 10.3390/molecules25081987
9. Thompson, K.H.; Orvig, C. Vanadium in diabetes: 100 years from Phase 0 to Phase I. *J. Inorg. Biochem.* **2006**, *100*, 1925-35. doi: 10.1016/j.jinorgbio.2006.08.016
10. Crans, D.C.; Henry, L.; Cardiff, G.; Posner, B.I. Developing vanadium as an antidiabetic or anticancer drug: A clinical and historical perspective. in: essential metals in medicine: therapeutic use and toxicity of metal ions in the clinic, Edited by Peggy L. Carver, Berlin, Boston: De Gruyter, 2019; 8, pp. 203-230. doi: 10.1515/9783110527872-014
11. Thompson, K.H.; Lichter, J.; LeBel, C.; Scaife, M.C.; McNeill, J.H.; Orvig, C. Vanadium treatment of type 2 diabetes: a view to the future. *J. Inorg. Biochem.* **2009**, *103*, 554-558. doi:10.1016/j.jinorgbio.2008.12.003
12. Soveid, M.; Dehghani, G.A.; Omrani, G.R. Long-term efficacy and safety of vanadium in the treatment of type 1 diabetes. *Arch. Iran Med.* **2013**, *16*, 408-411.
13. Kahn, S.E.; Cooper, M.E.; Del Prato, S. Pathophysiology and treatment of type 2 diabetes: perspectives on the past, present, and future. *Lancet* **2014**, *383*, 1068-83. doi: 10.1016/S0140-6736(13)62154-6



14. Kanwal, A.; Kanwar, N.; Bharati, S.; Srivastava, P.; Singh, S.P.; Amar, S. Exploring new drug targets for type 2 diabetes: success, challenges and opportunities. *Biomedicines* **2022**, *10*, 331. doi: 10.3390/biomedicines10020331
15. Treviño, S.; Díaz, A.; Sánchez-Lara, E.; Sanchez-Gaytan, B.L.; Perez-Aguilar, J.M.; González-Vergara, E. Vanadium in biological action: chemical, pharmacological aspects, and metabolic implications in diabetes mellitus. *Biol. Trace Elem. Res.* **2019**, *188*, 68-98. doi: 10.1007/s12011-018-1540-6
16. Crans, D.C.; Smee, J.J.; Gaidamauskas, E.; Yang, L. The chemistry and biochemistry of vanadium and the biological activities exerted by vanadium compounds. *Chem. Rev.* **2004**, *104*, 849-902. doi: 10.1021/cr020607t
17. Pendergrass, M.; Bertoldo, A.; Bonadonna, R.; Nucci, G.; Mandarino, L.; Cobelli, C.; DeFronzo, R.A. Muscle glucose transport and phosphorylation in type 2 diabetic, obese nondiabetic, and genetically predisposed individuals. *Am. J. Physiol. Endocrinol. Metab.* **2007**, *292*, E92-E100. doi:10.1152/ajpendo.00617.2005
18. DeFronzo, R.A.; Gunnarsson, R.; Björkman, O.; Olsson, M.; Wahren, J. Effects of insulin on peripheral and splanchnic glucose metabolism in noninsulin-dependent (type II) diabetes mellitus. *J. Clin. Invest.* **1985**, *76*, 149-155. doi:10.1172/JCI11938
19. Chait, A.; den Hartigh, L.J. Adipose tissue distribution, inflammation and its metabolic consequences, including diabetes and cardiovascular disease. *Front. Cardiovasc. Med.* **2020**, *7*, 22. doi:10.3389/fcvm.2020.00022
20. Chaudhury, A.; Duvoor, C.; Reddy Dendi, V.S.; Kraleti, S.; Chada, A.; Ravilla, R.; Marco, A.; Shekhawat, N.S.; Montales, M. T.; Kuriakose, K.; Sasapu, A.; Beebe, A.; Patil, N.; Musham, C.K.; Lohani, G.P.; Mirza, W. Clinical review of antidiabetic drugs: implications for type 2 diabetes mellitus management. *Front. Endocrinol. (Lausanne)*. **2017**, *8*, 6. doi:10.3389/fendo.2017.00006
21. Irving, E.; Stoker, A.W. Vanadium compounds as PTP Inhibitors. *Molecules* **2017**, *22*, 2269. doi: 10.3390/molecules22122269
22. Pandey, S.K.; Théberge, J.F.; Bernier, M.; Srivastava, A.K. Phosphatidylinositol 3-kinase requirement in activation of the ras/C-raf-1/MEK/ERK and p70(s6k) signaling cascade by the insulinomimetic agent vanadyl sulfate. *Biochemistry* **1999**, *38*, 14667-75. doi: 10.1021/bi9911886
23. Eleftheriou, P.; Geronikaki, A.; Petrou, A. PTP1b inhibition, a promising approach for the treatment of diabetes type II. *Curr. Top. Med. Chem.* **2019**, *19*, 246-263. doi: 10.2174/1568026619666190201152153
24. Mehdi, M.Z.; Pandey, S.K.; Théberge, J.F.; Srivastava, A.K. Insulin signal mimicry as a mechanism for the insulin-like effects of vanadium. *Cell Biochem. Biophys.* **2006**, *44*, 73-81. doi:10.1385/CBB:44:1:073
25. Pandey, S.K.; Chiasson, J.L.; Srivastava, A.K. Vanadium salts stimulate mitogen-activated protein (MAP) kinases and ribosomal S6 kinases. *Mol. Cell Biochem.* **1995**, *153*, 69-78. doi:10.1007/BF01075920
26. Neel, B.G.; Tonks, N.K. Protein tyrosine phosphatases in signal transduction. *Curr. Opin. Cell Biol.* **1997**, *9*, 193-204. doi: 10.1016/s0955-0674(97)80063-4
27. Xu, E.; Schwab, M.; Marette, A. Role of protein tyrosine phosphatases in the modulation of insulin signaling and their implication in the pathogenesis of obesity-linked insulin resistance. *Rev. Endocr. Metab. Disord.* **2014**, *15*, 79-97. doi: 10.1007/s11154-013-9282-4
28. Lu, L.; Zhu, M. Protein tyrosine phosphatase inhibition by metals and metal complexes. *Antioxid. Redox Signal* **2014**, *20*, 2210-24. doi: 10.1089/ars.2013.5720
29. Krüger, J.; Wellenhofer, E.; Meyborg, H.; Stawowy, P.; Östman, A.; Kintscher, U.; Kappert, K. Inhibition of Src homology 2 domain-containing phosphatase 1 increases insulin sensitivity in high-fat diet-induced insulin-resistant mice. *FEBS Open Bio.* **2016**, *6*, 179-89. doi: 10.1002/2211-5463.12000
30. Sevillano, J.; Sánchez-Alonso, M.G.; Pizarro-Delgado, J.; Ramos-Álvarez, M.D.P. Role of receptor protein tyrosine phosphatases (RPTPs) in insulin signaling and secretion. *Int. J. Mol. Sci.* **2021**, *22*, 5812. doi:10.3390/ijms22115812
31. Morioka, M.; Fukunaga, K.; Kawano, T.; Hasegawa, S.; Korematsu, K.; Kai, Y.; Hamada, J.; Miyamoto, E.; Ushio, Y. Serine/threonine phosphatase activity of calcineurin is inhibited by sodium orthovanadate and dithiothreitol reverses the inhibitory effect. *Biochem. Biophys. Res. Commun.* **1998**, *253*, 342-5. doi: 10.1006/bbrc.1998.9783
32. Semiz, S.; McNeill, J.H. Oral treatment with vanadium of Zucker fatty rats activates muscle glycogen synthesis and insulin-stimulated protein phosphatase-1 activity. *Mol. Cell Biochem.* **2002**, *236*, 123-31. doi: 10.1023/a:1016116700632
33. Honkanen, R.E.; Golden, T. Regulators of serine/threonine protein phosphatases at the dawn of a clinical era?. *Curr. Med. Chem.* **2002**, *9*, 2055-2075. doi:10.2174/0929867023368836
34. Copps, K.D.; White, M.F. Regulation of insulin sensitivity by serine/threonine phosphorylation of insulin receptor substrate proteins IRS1 and IRS2. *Diabetologia* **2012**, *55*, 2565-2582. doi: 10.1007/s00125-012-2644-8
35. Scrivens, P.J.; Alaoui-Jamali, M.A.; Giannini, G.; Wang, T.; Loignon, M.; Batist, G.; Sandor, V.A. Cdc25A-inhibitory properties and antineoplastic activity of bisperoxovanadium analogues. *Mol. Cancer Ther.* **2003**, *2*, 1053-9. PMID: 14578470
36. Liu, K.; Zheng, M.; Lu, R.; Du, J.; Zhao, Q.; Li, Z.; Li, Y.; Zhang, S. The role of CDC25C in cell cycle regulation and clinical cancer therapy: a systematic review. *Cancer Cell Int.* **2020**, *20*, 213. doi: 10.1186/s12935-020-01304-w
37. Pessoa, J.C.; Etcheverry, S.; Gambino, D. Vanadium compounds in medicine. *Coord. Chem. Rev.* **2015**, *301*, 24-48. doi:10.1016/j.ccr.2014.12.002
38. Crans, D.C.; Yang, L.; Haase, A.; Yang, X. "Health benefits of vanadium and its potential as an anticancer agent". In: Metallo-drugs: Development and action of anticancer agents, Edited by Astrid Sigel, Helmut Sigel, Eva Freisinger and Roland K.O. Sigel, Berlin, Boston: De Gruyter, 2018; 9, pp. 251-280. doi:10.1515/9783110470734-015
39. Crans, D.C.; Meade, T.J. Preface for the forum on metals in medicine and health: new opportunities and approaches to improving health. *Inorg. Chem.* **2013**, *52*, 12181-12183. doi:10.1021/ic402341n

40. Scior, T.; Guevara-García, A.; Bernard, P.; Do, Q.T.; Domeyer, D.; Laufer, S. Are vanadium compounds drugable? Structures and effects of antidiabetic vanadium compounds: a critical review. *Mini Rev. Med. Chem.* **2005**, *5*, 995-1008. doi: 10.2174/138955705774575264
41. Scior, T.; Guevara-García, J.A.; Do, Q.T.; Bernard, P.; Laufer, S. Why antidiabetic vanadium complexes are not in the pipeline of "Big Pharma" drug research? A critical review. *Curr. Med. Chem.* **2016**, *23*, 2874-2891. doi: 10.2174/0929867323666160321121138
42. Gryboś, R.; Paciorek, P.; Szklarzewicz, J.; Matoga, D.; Zabierowski, P.; Kazek, G. Novel vanadyl complexes of acetoacetanilide: Synthesis, characterization and inhibition of protein tyrosine phosphatase. *Polyhedron* **2013**, *49*, 100-104.
43. Zabierowski, P.; Szklarzewicz, J.; Gryboś, R.; Mordyl, B.; Nitek, W. Assemblies of salen-type oxidovanadium(IV) complexes: substituent effects and in vitro protein tyrosine phosphatase inhibition. *Dalton Trans.* **2014**, *43*, 17044-17053. doi: 10.1039/c4dt02344g
44. Szklarzewicz, J.; Jurowska, A.; Hodorowicz, M.; Gryboś, R.; Matoga, D. Role of co-ligand and solvent on properties of V(IV) oxido complexes with ONO Schiff bases. *J. Mol. Struct.* **2019**, *1180*, 839-848.
45. Gryboś, R.; Szklarzewicz, J.; Jurowska, A.; Hodorowicz, M. Properties, structure and stability of V(IV) hydrazide Schiff base ligand complex. *J. Mol. Struct.* **2018**, *1171*, 880-887.
46. Szklarzewicz, J.; Jurowska, A.; Matoga, D.; Kruczała, K.; Kazek, G.; Mordyl, B.; Sapa, J.; Papież, M. Synthesis, coordination properties and biological activity of vanadium complexes with hydrazone Schiff base ligands. *Polyhedron* **2020**, *185*, 1-13. doi.org/10.1016/j.molstruc.2018.06.077
47. Szklarzewicz, A.; Jurowska, M.; Hodorowicz, M.; Gryboś, R.; Kruczała, K.; Gluch-Lutwin, M.; Kazek, G. Vanadium complexes with salicylaldehyde-based Schiff base ligands-structure, properties and biological activity. *J. Coord. Chem.* **2020**, *73*, 986-1008. doi.org/10.1016/j.poly.2020.114589
48. Szklarzewicz, J.; Jurowska, A.; Hodorowicz, M.; Kazek, G.; Gluch-Lutwin, M.; Sapa, J. Ligand role on insulin-mimetic properties of vanadium complexes. Structural and biological studies. *Inorg. Chim. Acta* **2021**, *516*, 120135. doi.org/10.1080/00958972.2020.1755036
49. Szklarzewicz, J.; Jurowska, A.; Hodorowicz, M.; Kazek, G.; Mordyl, B.; Menaszek, E.; Sapa, J. Characterization and antidiabetic activity of salicylhydrazone Schiff base vanadium(IV) and (V) complexes. *Transit. Met. Chem.* **2021**, *46*, 201-217. doi.org/10.1007/s11243-020-00437-1
50. Jurowska, A.; Serafin, W.; Hodorowicz, M.; Kruczała, K.; Szklarzewicz, J. Vanadium precursors and the type of complexes formed with Schiff base ligand composed of 5-bromosalicylaldehyde and 2-hydroxybenzhydrazide—Structure and characterization. *Polyhedron* **2022**, *222*, 115903.
51. Jasińska, A.; Szklarzewicz, J.; Jurowska, A.; Hodorowicz, M.; Kazek, G.; Mordyl, B.; Gluch-Lutwin, M. V(III) and V(IV) Schiff base complexes as potential insulin-mimetic compounds—Comparison, characterization and biological activity. *Polyhedron* **2022**, *215*, 115682
52. Gryboś, R.; Szklarzewicz, J.; Matoga, D.; Kazek, G.; Stępniewski, M.; Krośniak, M.; Nowak, G.; Paciorek, P.; Zabierowski, P. Vanadium complexes with hydrazide-hydrazones, process for their preparation, pharmaceutical formulations and the use of thereof. World Patent No. WO2014073992A1. May 15, 2014.
53. Gryboś, R.; Szklarzewicz, J.; Matoga, D.; Kazek, G.; Stępniewski, M.; Krośniak, M.; Nowak, G.; Paciorek, P.; Zabierowski, P. Vanadium complexes with hydrazide-hydrazones, process for their preparation, pharmaceutical formulations and their use. PL Patent No. PL231079B1. November 07, 2012.
54. Kazek, G.; Gluch-Lutwin, M.; Mordyl, B.; Menaszek, E.; Szklarzewicz, J.; Gryboś, R.; Papież, M. Cell-based screening for identification of novel vanadium complexes with multidirectional activity relative to cells associated with metabolic disorders. *ST&I* **2019**, *4*, 47-54. doi.org/10.5604/01.3001.0013.1047
55. Kazek, G.; Gluch-Lutwin, M.; Mordyl, B.; Menaszek, E.; Sapa, J.; Szklarzewicz, J.; Gryboś, R.; Papież, M. Potentiation of adipogenesis and insulinomimetic effects of novel vanadium complex (N'-[(E)-(5-bromo-2-oxophenyl)methylidene]-4-methoxybenzohydrazide)oxido(1,10-phenanthroline)vanadium(IV) in 3T3-L1 cells. *ST&I* **2019**, *1*, 55-62. doi.org/10.5604/01.3001.0013.1048
56. ISO 10993-5:2009 Biological evaluation of medical devices. Part 5: Tests for in vitro cytotoxicity. International Organization for Standardization; Geneva, Switzerland: **2009**.
57. Dash, A.; Figler, R.A.; Sanyal, A.J.; Wamhoff, B.R. Drug-induced steatohepatitis. *Expert. Opin. Drug Metab. Toxicol.* **2017**, *13*, 193-204. doi:10.1080/17425255.2017.1246534
58. Peters, K.G.; Davis, M.G.; Howard, B.W.; Pokross, M.; Rastogi, V.; Diven, C.; Greis, K.D.; Eby-Wilkens, E.; Maier, M.; Evdokimov, A.; Soper, S.; Genbauffe, F. Mechanism of insulin sensitization by BMOV (bis maltolato oxo vanadium); unliganded vanadium (VO<sub>4</sub>) as the active component. *J. Inorg. Biochem.* **2003**, *96*, 321-30. doi: 10.1016/s0162-0134(03)00236-8
59. Cuncic, C.; Detich, N.; Ethier, D.; Tracey, A.S.; Gresser, M.J.; Ramachandran, C. Vanadate inhibition of protein tyrosine phosphatases in Jurkat cells: modulation by redox state. *J. Biol. Inorg. Chem.* **1999**, *4*, 354-359. doi:10.1007/s007750050322
60. Han, H.; Lu, L.; Wang, Q.; Zhu, M.; Yuan, C.; Xing, S.; Fu, X. Synthesis and evaluation of oxovanadium(IV) complexes of Schiff-base condensates from 5-substituted-2-hydroxybenzaldehyde and 2-substituted-benzenamine as selective inhibitors of protein tyrosine phosphatase 1B. *Dalton Trans.* **2012**, *41*, 11116-11124. doi:10.1039/c2dt30198a
61. Lu, L.; Gao, X.; Zhu, M.; Wang, S.; Wu, Q.; Xing, S.; Fu, X.; Liu, Z.; Guo, M. Exploration of biguanido-oxovanadium complexes as potent and selective inhibitors of protein tyrosine phosphatases. *Biomaterials* **2012**, *25*, 599-610. doi:10.1007/s10534-012-9548-4
62. Lu, L.; Wang, S.; Zhu, M.; Liu, Z.; Guo, M.; Xing, S.; Fu, X. Inhibition protein tyrosine phosphatases by an oxovanadium glutamate complex, Na<sub>2</sub>[VO(Glu)<sub>2</sub>(CH<sub>3</sub>OH)](Glu = glutamate). *Biomaterials* **2010**, *23*, 1139-1147. doi:10.1007/s10534-010-9363-8



63. Yuan, C.; Lu, L.; Gao, X.; Wu, Y.; Guo, M.; Li, Y.; Fu, X.; Zhu, M. Ternary oxovanadium(IV) complexes of ONO-donor Schiff base and polypyridyl derivatives as protein tyrosine phosphatase inhibitors: synthesis, characterization, and biological activities. *J. Biol. Inorg. Chem.* **2009**, *14*, 841-851. doi:10.1007/s00775-009-0496-6
64. Dubois, M.J.; Bergeron, S.; Kim, H.J.; Dombrowski, L.; Perreault, M.; Fournès, B.; Faure, R.; Olivier, M.; Beauchemin, N.; Shulman, G.I.; Siminovitch, K.A.; Kim, J.K.; Marette, A. The SHP-1 protein tyrosine phosphatase negatively modulates glucose homeostasis. *Nat. Med.* **2006**, *12*, 549-56. doi: 10.1038/nm1397
65. Bergeron, S.; Dubois, M.J.; Bellmann, K.; Schwab, M.; Larochelle, N.; Nalbantoglu, J.; Marette, A. Inhibition of the protein tyrosine phosphatase SHP-1 increases glucose uptake in skeletal muscle cells by augmenting insulin receptor signaling and GLUT4 expression. *Endocrinology* **2011**, *152*, 4581-8. doi: 10.1210/en.2011-1268
66. Xu, E.; Charbonneau, A.; Rolland, Y.; Bellmann, K.; Pao, L.; Siminovitch, K. A.; Neel, B.G.; Beauchemin, N.; Marette, A. Hepatocyte-specific Ptpn6 deletion protects from obesity-linked hepatic insulin resistance. *Diabetes* **2012**, *61*, 1949-1958. doi:10.2337/db11-1502
67. Qu, C.K. The SHP-2 tyrosine phosphatase: signaling mechanisms and biological functions. *Cell. Res.* **2000**, *10*, 279-88. doi: 10.1038/sj.cr.7290055
68. Yue, X.; Han, T.; Hao, W.; Wang, M.; Fu, Y. SHP2 knockdown ameliorates liver insulin resistance by activating IRS-2 phosphorylation through the AKT and ERK1/2 signaling pathways. *FEBS Open Bio* **2020**, *10*, 2578-2587. doi: 10.1002/2211-5463.12992
69. Nagata, N.; Matsuo, K.; Bettaieb, A.; Bakke, J.; Matsuo, I.; Graham, J.; Xi, Y.; Liu, S.; Tomilov, A.; Tomilova, N.; Gray, S.; Jung, D.Y.; Ramsey, J.J.; Kim, J.K.; Cortopassi, G.; Havel, P.J.; Haj, F.G. Hepatic Src homology phosphatase 2 regulates energy balance in mice. *Endocrinology* **2012**, *153*, 3158-3169. doi:10.1210/en.2012-1406
70. Kulas, D.T.; Zhang, W.R.; Goldstein, B.J.; Furlanetto, R.W.; Mooney, R.A. Insulin receptor signaling is augmented by antisense inhibition of the protein tyrosine phosphatase LAR. *J. Biol. Chem.* **1995**, *270*, 2435-8.
71. Zabolotny, J.M.; Kim, Y.B.; Peroni, O.D.; Kim, J.K.; Pani, M.A.; Boss, O.; Klamann, L.D.; Kamatkar, S.; Shulman, G.I.; Kahn, B.B.; Neel, B.G. Overexpression of the LAR (leukocyte antigen-related) protein-tyrosine phosphatase in muscle causes insulin resistance. *Proc. Natl. Acad. Sci. USA* **2001**, *98*, 5187-92. doi: 10.1073/pnas.071050398
72. Mooney, R.A.; LeVea, C.M. The leukocyte common antigen-related protein LAR: candidate PTP for inhibitory targeting. *Curr. Top. Med. Chem.* **2003**, *3*, 809-19. doi: 10.2174/1568026033452294
73. Gundhla, I.Z.; Walmsley, R.S.; Ugrinema, V.; Mnonopi, N. O.; Hosten, E.; Betz, R.; Frost, C. L.; Tshentu, Z. R.pH-metric chemical speciation modeling and studies of in vitro antidiabetic effects of bis[(imidazolyl)carboxylato]oxidovanadium(IV) complexes. *J. Inorg. Biochem.* **2015**, *145*, 11-18. doi:10.1016/j.jinorgbio.2014.12.019
74. Huyer, G.; Liu, S.; Kelly, J.; Moffat, J.; Payette, P.; Kennedy, B.; Tsaprailis, G.; Gresser, M.J.; Ramachandran, C. Mechanism of inhibition of protein-tyrosine phosphatases by vanadate and pervanadate. *J. Biol. Chem.* **1997**, *272*, 843-51. doi: 10.1074/jbc.272.2.843
75. Heo, Y.S.; Ryu, J.M.; Park, S.M.; Park, J.H.; Lee, H.C.; Hwang, K.Y.; Kim, J. Structural basis for inhibition of protein tyrosine phosphatases by Keggin compounds phosphomolybdate and phosphotungstate. *Exp. Mol. Med.* **2002**, *34*, 211-23. doi: 10.1038/emmm.2002.30
76. Zhang, Z.; Chen, F.; Huang, C.; Shi, X. Vanadate induces G2/M phase arrest in p53-deficient mouse embryo fibroblasts. *J. Environ. Pathol. Toxicol. Oncol.* **2002**, *21*, 223-231.
77. Liu, T.T.; Liu, Y.J.; Wang, Q.; Yang, X.G.; Wang, K. Reactive-oxygen-species-mediated Cdc25C degradation results in differential antiproliferative activities of vanadate, tungstate, and molybdate in the PC-3 human prostate cancer cell line. *J. Biol. Inorg. Chem.* **2012**, *17*, 311-20. doi: 10.1007/s00775-011-0852-1
78. Ajeawung, N.F.; Faure, R.; Jones, C.; Kamnasaran, D. Preclinical evaluation of dipotassium bisperoxo (picolinate) oxovanadate V for the treatment of pediatric low-grade gliomas. *Future Oncol.* **2013**, *9*, 1215-29. doi: 10.2217/fon.13.73
79. Saikia, G.; Gogoi, S.R.; Boruah, J.; Ram, B.; Begum, P.; Ahmed, K.; Sharma, M.; Ramakrishna, G.; Ramasarma, T.; Islam, N.S. Peroxo compounds of Vanadium(V) and Niobium(V) as potent inhibitors of calcineurin activity towards RII-Phosphopeptide. *ChemistrySelect* **2017**, *2*, 5838-5848. doi.org/10.1002/slct.201700935
80. Bhattacharyya, S.; Tracey, A.S. Vanadium(V) complexes in enzyme systems: aqueous chemistry, inhibition and molecular modeling in inhibitor design. *J. Inorg. Biochem.* **2001**, *85*, 9-13. doi:10.1016/s0162-0134(00)00229-4
81. Blau, H.M.; Chiu, C.P.; Webster, C. Cytoplasmic activation of human nuclear genes in stable heterocaryons. *Cell* **1983**, *32*, 1171-1180. doi:10.1016/0092-8674(83)90300-8
82. Mangnall, D.; Bruce, C.; Fraser, R.B. Insulin-stimulated glucose uptake in C2C12 myoblasts. *Biochem. Soc. Trans.* **1993**, *21*, 438S. doi:10.1042/bst021438s
83. Wong, C.Y.; Al-Salami, H.; Dass, C.R. C2C12 cell model: its role in understanding of insulin resistance at the molecular level and pharmaceutical development at the preclinical stage. *J. Pharm. Pharmacol.* **2020**, *72*, 1667-1693. doi:10.1111/jphp.13359
84. Shinde, U.A.; Sharma, G.; Goyal, R.K. In vitro insulin mimicking action of Bis(Maltolato) Oxovanadium (IV). *Indian J. Pharm. Sci.* **2004**, *66*, 392-395.
85. Lei, J.X.; Wang, J.; Huo, Y.; You, Z. 4-Fluoro-N'-(2-hydroxy-3-methoxybenzylidene) benzohydrazide and its Oxidovanadium(V) complex: Syntheses, crystal structures and insulin-enhancing activity. *Acta Chim. Slov.* **2016**, *63*, 670-677. doi:10.17344/acsi.2016.2589

86. Sun, Y.B.; Xie, Q.; Li, W.; Ding, Y.; Ye, Y.T. Synthesis, Crystal structures, and insulin enhancement of Vanadium(V) complexes derived from 2-Bromo-N'-(2-hydroxybenzylidene)benzohydrazide. *Synth. React. Inorg. Met. Org. Chem.* **2016**, *46*, 1613-1617. doi.org/10.1080/15533174.2015.1137039
87. Green, H.; Kehinde, O. Sublines of mouse 3T3 cells that accumulate lipid. *Cell* **1974**, *3*, 113-116. doi.org/10.1016/0092-8674(74)90126-3
88. Dufau, J.; Shen, J.X.; Couchet, M.; De Castro Barbosa, T.; Mejhert, N.; Massier, L.; Grisetti, E.; Mouisel, E.; Amri, E.Z.; Lauschke, V.M.; Rydén, M.; Langin, D. In vitro and ex vivo models of adipocytes. *Am. J. Physiol. Cell Physiol.* **2021**, *320*, C822-C841. doi:10.1152/ajpcell.00519.2020
89. DeFronzo, R.A. The triumvirate: beta-cell, muscle, liver. A collusion responsible for NIDDM. *Diabetes* **1988**, *37*, 667-687. doi:10.2337/diab.37.6.667
90. Abdul-Ghani, M.A.; DeFronzo, R.A. Pathogenesis of insulin resistance in skeletal muscle. *J. Biomed. Biotechnol.* **2010**, *2010*, 476279. doi:10.1155/2010/476279
91. Pereira, M.J.; Carvalho, E.; Eriksson, J.W.; Crans, D.C.; Aureliano, M. Effects of decavanadate and insulin enhancing vanadium compounds on glucose uptake in isolated rat adipocytes. *J. Inorg. Biochem.* **2009**, *103*, 1687-1692. doi:10.1016/j.jinorgbio.2009.09.015
92. Mueller, W.M.; Stanhope, K.L.; Gregoire, F.; Evans, J.L.; Havel, P.J. Effects of metformin and vanadium on leptin secretion from cultured rat adipocytes. *Obes. Res.* **2000**, *8*, 530-539. doi:10.1038/oby.2000.66
93. Cohen, N.; Halberstam, M.; Shlimovich, P.; Chang, C.J.; Shamon, H.; Rossetti, L. Oral vanadyl sulfate improves hepatic and peripheral insulin sensitivity in patients with non-insulin-dependent diabetes mellitus. *J. Clin. Invest.* **1995**, *95*, 2501-2509. doi:10.1172/JCI117951
94. Tsiani, E.; Bogdanovic, E.; Sorisky, A.; Nagy, L.; Fantus, I.G. Tyrosine phosphatase inhibitors, vanadate and pervanadate, stimulate glucose transport and GLUT translocation in muscle cells by a mechanism independent of phosphatidylinositol 3-kinase and protein kinase C. *Diabetes* **1998**, *47*, 1676-1686. doi:10.2337/diabetes.47.11.1676
95. Nunes, P.; Correia, I.; Cavaco, I.; Marques, F.; Pinheiro, T.; Aveilla, F.; Pessoa, J.C. Therapeutic potential of vanadium complexes with 1,10-phenanthroline ligands, quo vadis? Fate of complexes in cell media and cancer cells. *J. Inorg. Biochem.* **2021**, *217*, 111350. doi:10.1016/j.jinorgbio.2020.111350
96. Levina, A.; McLeod, A.I.; Pulte, A.; Aitken, J.B.; Lay, P.A. Biotransformations of antidiabetic vanadium prodrugs in mammalian cells and cell culture media: A XANES spectroscopic study. *Inorg. Chem.* **2015**, *54*, 6707-6718.
97. Rampersad, S.N. Multiple applications of Alamar Blue as an indicator of metabolic function and cellular health in cell viability bioassays. *Sensors (Basel)* **2012**, *12*, 12347-12360. doi:10.3390/s120912347
98. Mbatha, B.; Khathi, A.; Sibiyi, N.; Booysen, I.; Ngubane, P. A Dioxidovanadium complex cis-[VO<sub>2</sub>(obz)py] attenuates hyperglycemia in streptozotocin (STZ)-induced diabetic male sprague-dawley rats via increased GLUT4 and glycogen synthase expression in the skeletal muscle. *Evid. Based Complement. Alternat. Med.* **2022**, *2022*, 5372103. Published 2022 Jan 31. doi:10.1155/2022/5372103
99. Scalise, M.; Galluccio, M.; Console, L.; Pochini, L.; Indiveri, C. The human SLC7A5 (LAT1): The intriguing histidine/large neutral amino acid transporter and its relevance to human health. *Front. Chem.* **2018**, *6*, 243. doi:10.3389/fchem.2018.00243
100. Singh, N.; Ecker, G.F. Insights into the structure, function, and ligand discovery of the large neutral amino acid transporter 1, LAT1. *Int. J. Mol. Sci.* **2018**, *19*, 1278. doi:10.3390/ijms19051278
101. Klajner, M.; Licon, C.; Fetzer, L.; Hebraud, P.; Mellitzer, G.; Pfeffer, M.; Harlepp, S.; Gaiddon, C. Subcellular localization and transport kinetics of ruthenium organometallic anticancer compounds in living cells: a dose-dependent role for amino acid and iron transporters. *Inorg. Chem.* **2014**, *53*, 5150-5158. doi:10.1021/ic500250e
102. Minemura, T.; Lacy, W.W.; Crofford, O.B. Regulation of the transport and metabolism of amino acids in isolated fat cells. Effect of insulin and a possible role for adenosine 3',5'-monophosphate. *J. Biol. Chem.* **1970**, *245*, 3872-3881.
103. Nishitani, S.; Matsumura, T.; Fujitani, S.; Sonaka, I.; Miura, Y.; Yagasaki, K. Leucine promotes glucose uptake in skeletal muscles of rats. *Biochem. Biophys. Res. Commun.* **2002**, *299*, 693-696. doi:10.1016/s0006-291x(02)02717-1
104. Iwai, S.; Hasegawa, T.; Ikeda, H.O.; Tsujikawa, A. Branched chain amino acids promote ATP production via translocation of glucose transporters. *Invest. Ophthalmol. Vis. Sci.* **2022**, *63*, 7. doi:10.1167/iovs.63.9.7
105. Rhoads, D.E.; Ockner, R.K.; Peterson, N.A.; Raghupathy, E. Modulation of membrane transport by free fatty acids: inhibition of synaptosomal sodium-dependent amino acid uptake. *Biochemistry* **1983**, *22*, 1965-1970. doi:10.1021/bi00277a035
106. Rhoads, D.E.; Kaplan, M.A.; Peterson, N.A.; Raghupathy, E. Effects of free fatty acids on synaptosomal amino acid uptake systems. *J. Neurochem.* **1982**, *38*, 1255-1260. doi:10.1111/j.1471-4159.1982.tb07898.x
107. Byrne, C.D.; Targher, G. NAFLD: a multisystem disease. *J. Hepatol.* **2015**, *62*, S47-S64. doi:10.1016/j.jhep.2014.12.012
108. Huang, Y.; Liu, F.; Zhang, F.; Liu, P.; Xu, T.; Ding, W. Vanadium(IV)-chlorodipicolinate alleviates hepatic lipid accumulation by inducing autophagy via the LKB1/AMPK signaling pathway in vitro and in vivo. *J. Inorg. Biochem.* **2018**, *183*, 66-76. doi:10.1016/j.jinorgbio.2018.03.006
109. Wang, Y.; Chen, R.; Li, J.; Zeng, G.; Yuan, J.; Su, J.; Wu, C.; Lu, Z.; Zhang, F.; Ding, W. Vanadium(IV)-chlorodipicolinate protects against hepatic steatosis by ameliorating lipid peroxidation, endoplasmic reticulum stress, and inflammation. *Antioxidants (Basel)* **2022**, *11*, 1093. doi:10.3390/antiox11061093

110. Liu, Q.; Li, L.; Gao, L.; Li, C.; Huan, Y.; Lei, L.; Cao, H.; Li, L.; Gao, A.; Liu, S.; Shen, Z. Combination of bis ( $\alpha$ -furancarboxylato) oxovanadium (IV) and metformin improves hepatic steatosis through down-regulating inflammatory pathways in high-fat diet-induced obese C57BL/6J mice. *Basic Clin. Pharmacol. Toxicol.* **2021**, *128*, 747-757. doi:10.1111/bcpt.13573
111. Le, M.; Rathje, O.; Levina, A.; Lay, P.A. High cytotoxicity of vanadium(IV) complexes with 1,10-phenanthroline and related ligands is due to decomposition in cell culture medium. *J. Biol. Inorg. Chem.* **2017**, *22*, 663-672. doi:10.1007/s00775-017-1453-4
112. Levina, A.; Crans, D.C.; Lay, P.A. Speciation of metal drugs, supplements and toxins in media and bodily fluids controls in vitro activities. *Coord. Chem. Rev.* **2017**, *352*, 473-498. doi.org/10.1016/j.ccr.2017.01.002
113. Ścibior, A.; Zaporowska, H.; Ostrowski, J.; Banach, A. Combined effect of vanadium(V) and chromium(III) on lipid peroxidation in liver and kidney of rats. *Chem. Biol. Interact.* **2006**, *159*, 213-222. doi:10.1016/j.cbi.2005.11.008
114. Aureliano, M.; De Sousa-Coelho, A.L.; Dolan, C.C.; Roess, D.A.; Crans, D.C. Biological consequences of Vanadium effects on formation of reactive oxygen species and lipid peroxidation. *Int. J. Mol. Sciences* **2023**, *24*, 5382. doi.org/10.3390/ijms24065382
115. Hughes, T.B.; Flynn, N.; Dang, N.L.; Swamidass, S.J. Modeling the Bioactivation and Subsequent Reactivity of Drugs. *Chem Res Toxicol.* **2021**, *34*, 584-600. doi:10.1021/acs.chemrestox.0c00417
116. Dang, N.L.; Matlock, M.K.; Hughes, T.B.; Swamidass, S.J. The Metabolic Rainbow: Deep Learning Phase I Metabolism in Five Colors. *J Chem Inf Model.* **2020**, *60*, 1146-1164. doi:10.1021/acs.jcim.9b00836
117. Benedetto Tiz, D.; Bagnoli, L.; Rosati, O.; Marini, F.; Sancineto, L.; Santi, C. New Halogen-Containing Drugs Approved by FDA in 2021: An Overview on Their Syntheses and Pharmaceutical Use. *Molecules* **2022**, *27*, 1643. doi:10.3390/molecules27051643
118. Chiodi, D.; Ishihara, Y. "Magic Chloro": Profound Effects of the Chlorine Atom in Drug Discovery. *J Med Chem.* **2023**, *66*, 5305-5331. doi:10.1021/acs.jmedchem.2c02015
119. Murakami, H. A.; Uslan, C.; Haase, A. A.; Koehn, J. T.; Vieira, A. P.; Gaebler, D. J.; Hagan, J.; Beuning, C. N.; Proschogo, N.; Levina, A.; Lay, P. A.; Crans, D. C. Vanadium Chloro-Substituted Schiff Base Catecholate Complexes are Reducible, Lipophilic, Water Stable, and Have Anticancer Activities. *Inorg Chem.* **2022**, *61*, 20757-20773. doi:10.1021/acs.inorgchem.2c02557
120. Marzban, L.; Rahimian, R.; Brownsey, R.W.; McNeill, J.H. Mechanisms by which bis(maltolato)oxovanadium(IV) normalizes phosphoenolpyruvate carboxykinase and glucose-6-phosphatase expression in streptozotocin-diabetic rats in vivo. *Endocrinology* **2002**, *143*, 4636-4645. doi:10.1210/en.2002-220732
121. Valera, A.; Rodriguez-Gil, J.E.; Bosch, F. Vanadate treatment restores the expression of genes for key enzymes in the glucose and ketone bodies metabolism in the liver of diabetic rats. *J. Clin. Invest.* **1993**, *92*, 4-11. doi:10.1172/JCI116580
122. Ferber, S.; Meyerovitch, J.; Kriauciunas, K.M.; Kahn, C.R. Vanadate normalizes hyperglycemia and phosphoenolpyruvate carboxykinase mRNA levels in ob/ob mice. *Metabolism* **1994**, *43*, 1346-1354. doi:10.1016/0026-0495(94)90026-4
123. Mosseri, R.; Waner, T.; Shefi, M.; Shafir, E.; Meyerovitch, J. Gluconeogenesis in non-obese diabetic (NOD) mice: in vivo effects of vandate treatment on hepatic glucose-6-phosphatase and phosphoenolpyruvate carboxykinase. *Metabolism* **2000**, *49*, 321-325. doi:10.1016/s0026-0495(00)90132-x
124. Rines, A.K.; Sharabi, K.; Tavares, C.D.; Puigserver, P. Targeting hepatic glucose metabolism in the treatment of type 2 diabetes. *Nat. Rev. Drug Discov.* **2016**, *15*, 786-804. doi:10.1038/nrd.2016.151
125. Vardatsikos, G.; Mehdi, M.Z.; Srivastava, A.K. Bis(maltolato)-oxovanadium (IV)-induced phosphorylation of PKB, GSK-3 and FOXO1 contributes to its glucoregulatory responses (review). *Int. J. Mol. Med.* **2009**, *24*, 303-309. doi:10.3892/ijmm\_00000233
126. Mehdi, M.Z.; Srivastava, A.K. Organo-vanadium compounds are potent activators of the protein kinase B signaling pathway and protein tyrosine phosphorylation: mechanism of insulinomimesis. *Arch. Biochem. Biophys.* **2005**, *440*, 158-164. doi:10.1016/j.abb.2005.06.008
127. Leclercq, I.A.; Da Silva Morais, A.; Schroyen, B.; Van Hul, N.; Geerts, A. Insulin resistance in hepatocytes and sinusoidal liver cells: mechanisms and consequences. *J. Hepatol.* **2007**, *47*, 142-156. doi:10.1016/j.jhep.2007.04.002
128. Coulibaly, S.; McPherson, K.; Nair, S.; Ruff, D.; Stapleton, S.R. Evaluation of the effectiveness of the insulin-mimetics, selenium and vanadium, in insulin-resistance in primary hepatocytes. *FASEB J.* **2011**, *25*, 530.5-530.5. doi.org/10.1096/fasebj.25.1\_supplement.530.5
129. Bulger, D.A.; Conley, J.; Conner, S.H.; Majumdar, G.; Solomon, S.S. Role of PTEN in TNF $\alpha$  induced insulin resistance. *Biochem. Biophys. Res. Commun.* **2015**, *461*, 533-536. doi:10.1016/j.bbrc.2015.04.063
130. Boccato Payolla, F.; Andrade Aleixo N.; Resende Nogueira, F.A.; Massabni, A.C. Estudos in vitro da Atividade Antitumoral de Complexos de Vanádio com Ácidos Órotico e Glutâmico. *Rev. Bras. Cancerol.* [Internet]. **2020** Jan. 29 [cited 2023 Apr. 14];66(1):e-04649. doi.org/10.32635/2176-9745.RBC.2020v66n1.649
131. Levina, A.; Crans, D.C.; Lay, P.A. Advantageous reactivity of unstable metal complexes: Potential applications of metal-based anticancer drugs for intratumoral injections. *Pharmaceutics* **2022**, *14*, 790. doi:10.3390/pharmaceutics14040790
132. Szlasa, W.; Zendran, I.; Zalesińska, A.; Tarek, M.; Kulbacka, J. Lipid composition of the cancer cell membrane. *J. Bioenerg. Biomembr.* **2020**, *52*, 321-342. doi:10.1007/s10863-020-09846-4
133. Welte, S.; Baringhaus, K.H.; Schmider, W.; Müller, G.; Petry, S.; Tennagels, N. 6,8-Difluoro-4-methylumbiliferyl phosphate: a fluorogenic substrate for protein tyrosine phosphatases. *Anal. Biochem.* **2005**, *338*, 32-8. doi: 10.1016/j.ab.2004.11.047
134. Pastula, C.; Johnson, I.; Beechem, J.M.; Patton, W.F. Development of fluorescence-based selective assays for serine/threonine and tyrosine phosphatases. *Comb. Chem. High Throughput Screen.* **2003**, *6*, 341-6. doi: 10.2174/138620703106298590
135. Wensaas, A.J.; Rustan, A.C.; Lövestedt, K.; Kull, B.; Wikström, S.; Drevon, C.A.; Hallén, S. Cell-based multiwell assays for the detection of substrate accumulation and oxidation. *J. Lipid Res.* **2007**, *48*, 961-7. doi: 10.1194/jlr.D600047-JLR200

136. Yamamoto, N.; Ueda-Wakagi, M.; Sato, T.; Kawasaki, K.; Sawada, K.; Kawabata, K.; Akagawa, M.; Ashida, H. Measurement of glucose uptake in cultured cells. *Curr. Protoc. Pharmacol.* **2015**, *71*, 12.14.1-12.14.26. doi:10.1002/0471141755.ph1214s71
137. Pither, R.; Game, S.; Davis, J.; Katz, M.; McLane, J. The use of Cytostar-T™ scintillating microplates to monitor insulin-dependent glucose uptake by 3T3-L1 adipocytes. *Exp. Clin. Endocrinol. Diabetes* **1996**, *104*, 115-116. doi: 10.1055/s-0029-1211591
138. Tanti, J.F.; Cormont, M.; Grémeaux, T.; Le Marchand-Brustel, Y. Assays of glucose entry, glucose transporter amount, and translocation. *Methods Mol. Biol.* **2001**, *155*, 157-65. doi: 10.1385/1-59259-231-7:157
139. Gómez-Lechón, M.J.; Donato, M.T.; Martínez-Romero, A.; Jiménez, N.; Castell, J.V.; O'Connor, J.E. A human hepatocellular in vitro model to investigate steatosis. *Chem. Biol. Interact.* **2007**, *165*, 106-16. doi: 10.1016/j.cbi.2006.11.004
140. Ricchi, M.; Odoardi, M.R.; Carulli, L.; Anzivino, C.; Ballestri, S.; Pinetti, A.; Fantoni, L.I.; Marra, F.; Bertolotti, M.; Banni, S.; Lonardo, A.; Carulli, N.; Loria, P. Differential effect of oleic and palmitic acid on lipid accumulation and apoptosis in cultured hepatocytes. *J. Gastroenterol. Hepatol.* **2009**, *24*, 830-40. doi: 10.1111/j.1440-1746.2008.05733.x
141. Okamoto, T.; Kanemoto, N.; Ban, T.; Sudo, T.; Nagano, K.; Niki, I. Establishment and characterization of a novel method for evaluating gluconeogenesis using hepatic cell lines, H4IIE and HepG2. *Arch. Biochem. Biophys.* **2009**, *491*, 46-52. doi: 10.1016/j.abb.2009.09.015
142. García-Ruiz, I.; Solís-Muñoz, P.; Gómez-Izquierdo, E.; Muñoz-Yagüe, M.T.; Valverde, A.M.; Solís-Herruzo, J.A. Protein-tyrosine phosphatases are involved in interferon resistance associated with insulin resistance in HepG2 cells and obese mice. *J. Biol. Chem.* **2012**, *287*, 19564-73. doi: 10.1074/jbc.M112.342709
143. Li, M.; Han, Z.; Bei, W.; Rong, X.; Guo, J.; Hu, X. Oleanolic acid attenuates insulin resistance via NF-κB to regulate the IRS1-GLUT4 pathway in HepG2 cells. *Evid. Based Complement. Alternat. Med.* **2015**, *2015*, 643102. doi: 10.1155/2015/643102
144. Olsson, T.; Gulliksson, H.; Palmeborn, M.; Bergström, K.; Thore, A. Leakage of adenylate kinase from stored blood cells. *J. Appl. Biochem.* **1983**, *5*, 437-45.
145. Eglen, R.M.; Reisine, T.; Roby, P.; Rouleau, N.; Illy, C.; Bossé, R.; Bielefeld, M. The use of AlphaScreen technology in HTS: current status. *Curr. Chem. Genomics.* **2008**, *1*, 2-10. doi: 10.2174/1875397300801010002

**Disclaimer/Publisher's Note:** The statements, opinions and data contained in all publications are solely those of the individual author(s) and contributor(s) and not of MDPI and/or the editor(s). MDPI and/or the editor(s) disclaim responsibility for any injury to people or property resulting from any ideas, methods, instructions or products referred to in the content.